Available online at www.sciencedirect.com

SciVerse ScienceDirect

Nuclear Physics B 860 (2012) 207–244

NUCLEAR PHYSICS B

www.elsevier.com/locate/nuclphysb

NMSSM Higgs benchmarks near 125 GeV

S.F. King [a], M. Mühlleitner [b,*], R. Nevzorov [c,1]

[a] *School of Physics and Astronomy, University of Southampton, Southampton, SO17 1BJ, UK*
[b] *Institute for Theoretical Physics, Karlsruhe Institute of Technology, 76128 Karlsruhe, Germany*
[c] *Department of Physics and Astronomy, University of Hawaii, Honolulu, HI 96822, Hawaii, United States*

Received 21 January 2012; accepted 17 February 2012

Available online 3 March 2012

Abstract

The recent LHC indications of a SM-like Higgs boson near 125 GeV are consistent not only with the Standard Model (SM) but also with Supersymmetry (SUSY). However naturalness arguments disfavour the Minimal Supersymmetric Standard Model (MSSM). We consider the Next-to-Minimal Supersymmetric Standard Model (NMSSM) with a SM-like Higgs boson near 125 GeV involving relatively light stops and gluinos below 1 TeV in order to satisfy naturalness requirements. We are careful to ensure that the chosen values of couplings do not become non-perturbative below the grand unification (GUT) scale, although we also examine how these limits may be extended by the addition of extra matter to the NMSSM at the two-loop level. We then propose four sets of benchmark points corresponding to the SM-like Higgs boson being the lightest or the second lightest Higgs state in the NMSSM or the NMSSM-with-extra-matter. With the aid of these benchmark points we discuss how the NMSSM Higgs boson near 125 GeV may be distinguished from the SM Higgs boson in future LHC searches.

1. Introduction

The ATLAS and CMS Collaborations have recently presented the first indication for a Higgs boson with a mass in the region ∼124–126 GeV [1,2]. An excess of events is observed by the ATLAS experiment for a Higgs boson mass hypothesis close to 126 GeV with a maximum local statistical significance of 3.6σ above the expected SM background and by the CMS experiment

* Corresponding author.
E-mail addresses: king@soton.ac.uk (S.F. King), maggie@particle.uni-karlsruhe.de (M. Mühlleitner), nevzorov@phys.hawaii.edu (R. Nevzorov).
[1] On leave of absence from the Theory Department, ITEP, Moscow, Russia.

0550-3213/$ – see front matter
doi:10.1016/j.nuclphysb.2012.02.010

at 124 GeV with 2.6σ maximum local significance. If the ATLAS and CMS signals are combined the statistical significance increases, but is still less than the 5σ required to claim a discovery. Interestingly, the ATLAS signal in the $\gamma\gamma$ decay channel by itself has a local significance of 2.8σ whereas a SM-like Higgs boson would only have a significance of half this value, leading to speculation that the observed Higgs boson is arising from beyond SM physics. In general, these results have generated much excitement in the community, and already there are a number of papers discussing the implications of such a Higgs boson [3–7].

In the Minimal Supersymmetric Standard Model (MSSM) the lightest Higgs boson is lighter than about 130–135 GeV, depending on top squark parameters (see e.g. [8] and references therein). A 125 GeV SM-like Higgs boson is consistent with the MSSM in the decoupling limit. In the limit of decoupling the light Higgs mass is given by

$$m_h^2 \approx M_Z^2 \cos^2 2\beta + \Delta m_h^2, \tag{1.1}$$

where Δm_h^2 is dominated by loops of heavy top quarks and top squarks and $\tan\beta$ is the ratio of the vacuum expectation values (VEVs) of the two Higgs doublets introduced in the MSSM Higgs sector. At large $\tan\beta$, we require $\Delta m_h \approx 85$ GeV which means that a very substantial loop contribution, nearly as large as the tree-level mass, is needed to raise the Higgs boson mass to 125 GeV. The rather complicated parameter dependence has been studied in [4] where it was shown that, with "maximal stop mixing", the lightest stop mass must be $m_{\tilde{t}_1} \gtrsim 500$ GeV (with the second stop mass considerably larger) in the MSSM in order to achieve a 125 GeV Higgs boson. However one of the motivations for SUSY is to solve the hierarchy or fine-tuning problem of the SM [9]. It is well known that such large stop masses typically require a tuning at least of order 1% in the MSSM, depending on the parameter choice and the definition of fine-tuning [10].

In the light of such fine-tuning considerations, it has been known for some time, even after the LEP limit on the Higgs boson mass of 114 GeV, that the fine-tuning of the MSSM could be ameliorated in the Next-to-Minimal Supersymmetric Standard Model (NMSSM) [11]. With a 125 GeV Higgs boson, this conclusion is greatly strengthened and the NMSSM appears to be a much more natural alternative. In the NMSSM, the spectrum of the MSSM is extended by one singlet superfield [12–14] (for reviews see [15,16]). In the NMSSM the supersymmetric Higgs mass parameter μ is promoted to a gauge-singlet superfield, S, with a coupling to the Higgs doublets, $\lambda S H_u H_d$, that is perturbative up to unified scales. In the pure NMSSM values of $\lambda \sim 0.7$ do not spoil the validity of perturbation theory up to the GUT scale only providing $\tan\beta \gtrsim 4$, however the presence of additional extra matter [17] allows smaller values of $\tan\beta$ to be achieved. The maximum mass of the lightest Higgs boson is

$$m_h^2 \approx M_Z^2 \cos^2 2\beta + \lambda^2 v^2 \sin^2 2\beta + \Delta m_h^2 \tag{1.2}$$

where here we use $v = 174$ GeV. For $\lambda v > M_Z$, the tree-level contributions to m_h are maximized for moderate values of $\tan\beta$ rather than by large values of $\tan\beta$ as in the MSSM. For example, taking $\lambda = 0.7$ and $\tan\beta = 2$, these tree-level contributions raise the Higgs boson mass to about 112 GeV, and $\Delta m_h \gtrsim 55$ GeV is required. This is to be compared to the MSSM requirement $\Delta m_h \gtrsim 85$ GeV. The difference between these two values (numerically about 30 GeV) is significant since Δm_h depends logarithmically on the stop masses as well as receiving an important contribution from stop mixing. This means for example, that, unlike the MSSM, in the case of the NMSSM maximal stop mixing is not required to get the Higgs heavy enough.

The NMSSM has in fact several attractive features as compared to the widely studied MSSM. Firstly, the NMSSM naturally solves in an elegant way the so-called μ problem [18] of the MSSM, namely that the phenomenologically required value for the supersymmetric Higgsino

mass μ in the vicinity of the electroweak or SUSY breaking scale is not explained. This is automatically achieved in the NMSSM, since an effective μ-parameter is dynamically generated when the singlet Higgs field acquires a vacuum expectation value of the order of the SUSY breaking scale, leading to a fundamental Lagrangian that contains no dimensionful parameters apart from the soft SUSY breaking terms. Secondly, as compared to the MSSM, the NMSSM can induce a richer phenomenology in the Higgs and neutralino sectors, both in collider and dark matter (DM) experiments. For example, heavier Higgs states can decay into lighter ones with sizable rates [19–30]. In addition, a new possibility appears for achieving the correct cosmological relic density [31] through the so-called "singlino", i.e. the fifth neutralino of the model, which can have weaker-than-usual couplings to SM particles. The NMSSM Higgs boson near 125 GeV may also have significantly different properties than the SM Higgs boson [5,6], as we shall discuss in some detail here. Thirdly, as already discussed at length above, the NMSSM requires less fine-tuning than the MSSM [11].

Since the NMSSM (as in the case for the MSSM) has a rich parameter space, it is convenient to consider the standard approach of so-called "benchmark points" in the SUSY parameter space. These consist of a few "discrete" parameter configurations of a given SUSY model, which in our case are supposed to lead to typical phenomenological features. Using discrete points avoids scanning the entire parameter space, focusing instead on representative choices that reflect the new interesting features of the model, such as new signals, peculiar mass spectra, and so on. A reduced number of points can then be subject to full experimental investigation, without loss of substantial theoretical information. While several such benchmark scenarios have been devised for the MSSM [32,33] and thoroughly studied in both the collider and the DM contexts, and even for the NMSSM [34], these need to be revised in the light of the 125 GeV Higgs signal. The motivation for finding such NMSSM benchmarks is to enable the characteristics of the NMSSM Higgs boson near 125 GeV to be identified, so that it may eventually be resolved from that of the SM Higgs boson.

In this paper we present a set of NMSSM benchmark points with a SM-like Higgs boson mass near 125 GeV, focussing on the cases where both stop masses are as light as possible in order to reduce the fine-tuning, in accordance with the above discussion. The tools to calculate the Higgs and SUSY particle spectra in the NMSSM, in particular `NMSSMTools`, have been available for some time [21,35,36], although these will be supplemented by other codes as discussed later. The goal of the paper is to firstly find NMSSM benchmark points which contain a 125 GeV SM-like Higgs boson and in addition involve relatively light stops. Since the stops receive radiative corrections to their masses from gluinos, we shall also require relatively light gluinos as well as having as small an effective $\mu_{\rm eff}$ parameter ($\mu_{\rm eff} = \lambda\langle S\rangle$) as possible [37]. Having relatively light stops (and sbottoms), care has to be taken not to be in conflict with direct searches at the Tevatron and recent searches at the LHC. In addition, light stops appearing in the triangle loop diagrams can significantly affect Higgs production via gluon fusion as well as Higgs decay into two photons. Once a parameter set leading to a 125 GeV NMSSM Higgs boson has been found it has to be checked if the production cross-sections and branching ratios are such that they lead to a total Higgs production cross-section times branching ratios which is compatible with the LHC searches. The obtained branching ratios can be used to ultimately distinguish the NMSSM Higgs boson from the SM Higgs state. However, we do not attempt to simulate the LHC search strategies, our goal being the much more modest one of providing benchmarks with different characteristic types of NMSSM Higgs bosons, which can eventually be studied in more detail. The types of benchmark points considered here all involve relatively large values of $\lambda > 0.5$ and small values of $\tan\beta \leqslant 3$, in order to allow for the least fine-tuning possible involving light

stops as discussed above. However we are careful to respect the perturbativity bounds on λ up to the GUT scale, either for the pure NMSSM, or the NMSSM supplemented by three copies of extra $SU(5)$ $5+\bar{5}$ states, where such bounds are calculated using two-loop renormalisation group equations (RGEs). We find that the NMSSM Higgs boson near 125 GeV can come in many guises. It may be very SM-like, practically indistinguishable from the SM Higgs boson. Or it may have different Higgs production cross-sections and widely varying decay branching ratios which enable it to be resolved from the SM Higgs boson. The key distinguishing feature of the NMSSM, compared to the MSSM, is the presence of the singlet S which may mix into the 125 GeV Higgs mass state to a greater or lesser extent. As the singlet component of the 125 GeV Higgs boson is increased, either the H_d or H_u components (or both) must be reduced. If the H_d component is reduced then this reduces the decay rate into bottom quarks and can allow other rare decays like $\gamma\gamma$ to have larger branching ratios [6]. In addition there is the effect of SUSY particle and charged Higgs boson loops in the Higgs coupling to photons which can increase or decrease the rate of decays into $\gamma\gamma$.

In order to put the present work in context, it is worth to emphasise that this is the first paper to propose "natural" (i.e. involving light stops) NMSSM benchmark points with a SM-like Higgs boson near 125 GeV. For example, the previous NMSSM benchmark paper [34] was concerned with the constrained NMSSM which does not allow light stops consistent with current LHC SUSY limits. Also, while this paper was being prepared there have appeared a number of other related papers, none of which however are focussed on the task of providing benchmark points. For example, the results in [4] were mainly concerned with fine-tuning issues in SUSY models with a $\lambda S H_u H_d$ coupling for a SM-like Higgs boson near 126 GeV and the actual NMSSM was strictly not considered since an explicit μ term was included whereas the trilinear singlet coupling $\frac{\kappa}{3}S^3$ was neglected. By contrast another recent paper [5] did consider the actual NMSSM although no benchmarks were proposed. As this paper was being finalised, further dedicated NMSSM papers with a Higgs boson near 125 GeV have started to appear, in particular [6] in which the two photon enhancement was emphasised but without benchmark points, and [7] where (versions of) the constrained NMSSM were considered. It should be clear that the present paper is both complementary and contemporary to all these papers.

The layout of the remainder of the paper is as follows. In Section 2 we discuss the MSSM and fine-tuning, showing that it leads to constraints on the mass of the heavier stop quark. In Section 3 we briefly review the NMSSM, and provide perturbativity limits of the coupling λ depending on the coupling κ as well as $\tan\beta$. We show how the limit on λ may be increased if there is extra matter in the SUSY desert. Section 4 is concerned with constraints from Higgs searches, SUSY particle searches and Dark Matter. Section 5 contains the four sets of NMSSM Higgs benchmarks near 125 GeV that we are proposing, including the Higgs production cross-sections and branching ratios which ultimately will enable it to be distinguished from the SM Higgs boson. Section 6 summarises and concludes the paper. Appendix A contains the two-loop RGEs from which the perturbativity bounds on λ were obtained.

2. The MSSM

The superpotential of the MSSM is given, in terms of (hatted) superfields, by

$$\mathcal{W} = \mu \widehat{H}_u \widehat{H}_d + h_t \widehat{Q}_3 \widehat{H}_u \widehat{t}^c_R - h_b \widehat{Q}_3 \widehat{H}_d \widehat{b}^c_R - h_\tau \widehat{L}_3 \widehat{H}_d \widehat{\tau}^c_R, \tag{2.3}$$

in which only the third generation fermions have been included (with possible neutrino Yukawa couplings have been set to zero), and $\widehat{Q}_3$, $\widehat{L}_3$ stand for superfields associated with the (t, b) and (τ, ν_τ) $SU(2)$ doublets.

The soft SUSY breaking terms consist of the scalar mass terms for the Higgs and sfermion scalar fields which, in terms of the fields corresponding to the complex scalar components of the superfields, are given by

$$-\mathcal{L}_{\text{mass}} = m_{H_u}^2 |H_u|^2 + m_{H_d}^2 |H_d|^2 + m_{\tilde{Q}_3}^2 |\tilde{Q}_3^2| + m_{\tilde{t}_R}^2 |\tilde{t}_R^2| + m_{\tilde{b}_R}^2 |\tilde{b}_R^2| + m_{\tilde{L}_3}^2 |\tilde{L}_3^2| + m_{\tilde{\tau}_R}^2 |\tilde{\tau}_R^2|, \tag{2.4}$$

and the trilinear interactions between the sfermion and Higgs fields,

$$-\mathcal{L}_{\text{tril}} = B\mu H_u H_d + h_t A_t \tilde{Q}_3 H_u \tilde{t}_R^c - h_b A_b \tilde{Q}_3 H_d \tilde{b}_R^c - h_\tau A_\tau \tilde{L}_3 H_d \tilde{\tau}_R^c + \text{h.c.} \tag{2.5}$$

The tree-level MSSM Higgs potential is given by

$$V_0 = m_1^2 |H_d|^2 + m_2^2 |H_u|^2 - m_3^2 (H_d H_u + \text{h.c.}) + \frac{g_2^2}{8} \left(H_d^+ \sigma_a H_d + H_u^+ \sigma_a H_u\right)^2 + \frac{g'^2}{8} \left(|H_d|^2 - |H_u|^2\right)^2 \tag{2.6}$$

where $g' = \sqrt{3/5} g_1$, g_2 and g_1 are the low energy (GUT normalised) $SU(2)_W$ and $U(1)_Y$ gauge couplings, $m_1^2 = m_{H_d}^2 + \mu^2$, $m_2^2 = m_{H_u}^2 + \mu^2$ and $m_3^2 = -B\mu$.

In the MSSM, at the 1-loop level, stops contribute to the Higgs boson mass and three more parameters become important, the stop soft masses, $m_{\tilde{Q}_3}$ and $m_{\tilde{t}_R}$, and the stop mixing parameter

$$X_t = A_t - \mu \cot \beta. \tag{2.7}$$

The dominant one-loop contribution to the Higgs boson mass depends on the geometric mean of the stop masses, $m_{\tilde{t}}^2 = m_{\tilde{Q}_3} m_{\tilde{t}_R}$, and is given by,

$$\Delta m_h^2 \approx \frac{3}{(4\pi)^2} \frac{m_t^4}{v^2} \left[\ln \frac{m_{\tilde{t}}^2}{m_t^2} + \frac{X_t^2}{m_{\tilde{t}}^2} \left(1 - \frac{X_t^2}{12 m_{\tilde{t}}^2}\right)\right]. \tag{2.8}$$

The Higgs mass is sensitive to the degree of stop mixing through the second term in the brackets, and is maximized for $|X_t| = X_t^{\text{max}} = \sqrt{6} m_{\tilde{t}}$, which was referred to as "maximal mixing" above.

The fine-tuning in the MSSM can be simply understood by examining the leading one-loop correction to the Higgs potential,

$$\Delta V = \frac{3}{32\pi^2} \left[m_{\tilde{t}_1}^4 \left(\ln \frac{m_{\tilde{t}_1}^2}{Q^2} - \frac{3}{2} \right) + m_{\tilde{t}_2}^4 \left(\ln \frac{m_{\tilde{t}_2}^2}{Q^2} - \frac{3}{2} \right) - 2 m_t^4 \left(\ln \frac{m_t^2}{Q^2} - \frac{3}{2} \right) \right], \tag{2.9}$$

where the two stop masses are,

$$m_{\tilde{t}_{1,2}}^2 = \frac{1}{2} \left(m_{\tilde{Q}_3}^2 + m_{\tilde{t}_R}^2 + 2 m_t^2 + \frac{1}{2} M_Z^2 \cos 2\beta \mp \sqrt{\left(m_{\tilde{Q}_3}^2 - m_{\tilde{t}_R}^2 + \frac{4}{3} M_W^2 \cos 2\beta - \frac{5}{6} M_Z^2 \cos 2\beta \right)^2 + 4 m_t^2 X_t^2} \right). \tag{2.10}$$

The fine-tuning originates from the fact that $\Delta V \gg v^4$, where $v = 174$ GeV is the combined Higgs VEV. By considering the minimization conditions for the Higgs potential, one finds

$$\mu^2 + \frac{1}{2}M_Z^2 + \Delta = \frac{(m_{H_d}^2 - m_{H_u}^2 \tan^2\beta)}{\tan^2\beta - 1}, \tag{2.11}$$

where

$$\begin{aligned}\Delta = \frac{1}{\tan^2\beta - 1}\Bigg\{ & \frac{3m_t^2}{16\pi^2 v^2 \cos^2\beta}\big[f(m_{\tilde{t}_2}) + f(m_{\tilde{t}_1}) - 2f(m_t)\big] \\ & - \frac{3M_Z^2}{64\pi^2 v^2 \cos^2\beta}\big[f(m_{\tilde{t}_2}) + f(m_{\tilde{t}_1})\big] \\ & - \frac{3}{32\pi^2 v^2 \cos^2\beta}\left(\frac{4}{3}M_W^2 - \frac{5}{6}M_Z^2\right)\big[f(m_{\tilde{t}_2}) - f(m_{\tilde{t}_1})\big]\cos 2\theta_t \\ & + \left(\frac{3(m_{\tilde{t}_2}^2 - m_{\tilde{t}_1}^2)}{64\pi^2 v^2 \cos^2\beta}\sin^2 2\theta_t + \frac{3m_t\mu \sin 2\theta_t}{8\pi^2 v^2 \sin 2\beta}\right)\big[f(m_{\tilde{t}_2}) - f(m_{\tilde{t}_1})\big]\Bigg\}. \end{aligned} \tag{2.12}$$

In Eq. (2.12) θ_t is the mixing angle in the stop sector given by

$$\sin 2\theta_t = \frac{2m_t X_t}{(m_{\tilde{t}_2}^2 - m_{\tilde{t}_1}^2)}, \tag{2.13}$$

whereas

$$f(m) = m^2\left(\ln\frac{m^2}{Q^2} - 1\right).$$

Here we set the renormalisation scale $Q = m_t$. From Eq. (2.11) one can see that in order to avoid tuning,

$$\Delta \lesssim \frac{1}{2}M_Z^2. \tag{2.14}$$

This shows that both stop masses must be light to avoid tuning. For example, defining $\Delta_{II} = 2 \cdot \Delta / M_Z^2$ the absence of any tuning requires $\Delta_{II} \lesssim 1$. This in turn requires the heavier stop mass to be below about 500 GeV as illustrated in Fig. 1. This constraint on the heavier stop mass has not been emphasised in the literature, where often the focus of attention is on the lightest stop mass.

It has been noted that large or maximal stop mixing is associated with large fine-tuning. This also follows from Fig. 1 and Eq. (2.12). Indeed, Fig. 1 demonstrates that the contribution of one-loop corrections to Eq. (2.11) increases when the mixing angle in the stop sector becomes larger. In fact when θ_t is close to $\pi/4$ the last term in Eq. (2.12) gives the dominant contribution to Δ enhancing the overall contribution of loop corrections in the minimization condition (2.11) which determines the mass of the Z-boson.

Eq. (2.11) also indicates that in order to avoid tuning one has to ensure that the parameter μ has a reasonably small value. To avoid tuning entirely one should expect μ to be less than M_Z. However, so small values of the parameter μ are ruled out by chargino searches at LEP. Therefore in our analysis we allow the effective μ_{eff} parameter to be as large as 200 GeV that does not result in enormous fine-tuning.

3. The NMSSM

In this paper, we only consider the NMSSM with a scale invariant superpotential. Alternative models known as the minimal non-minimal supersymmetric SM (MNSSM), new minimally-

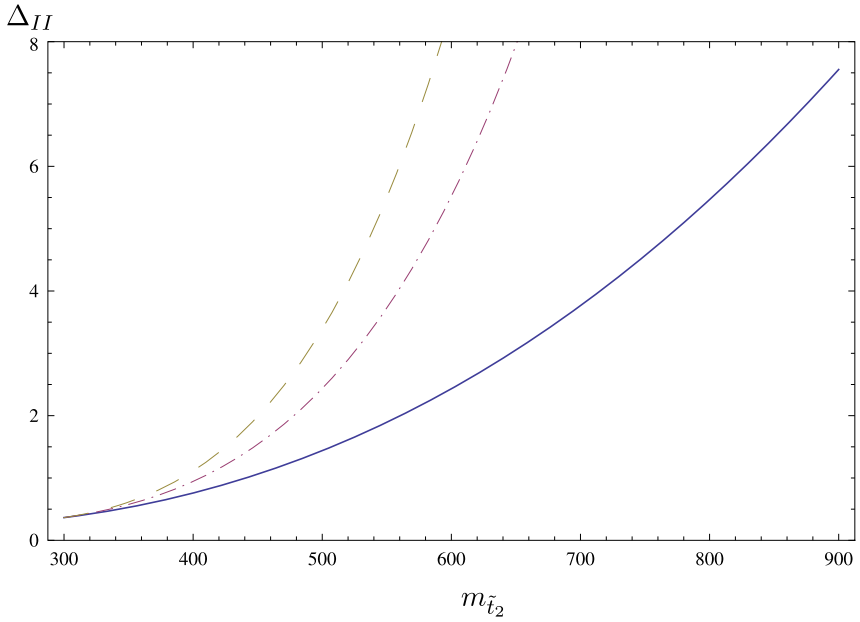

Fig. 1. The contribution of one-loop corrections to Eq. (2.11) as a function of the mass of the heaviest stop $m_{\tilde{t}_2}$ for $\tan\beta = 10$, $\mu = 200$ GeV, $Q = m_t = 165$ GeV and $m_{\tilde{t}_1} = 300$ GeV. Here $\Delta_{II} = 2 \cdot \Delta / M_Z^2$. Solid, dashed–dotted and dashed lines correspond to the mixing angle in the stop sector $\theta_t = 0, \pi/8$ and $\pi/4$, respectively.

extended supersymmetric SM or nearly-minimal supersymmetric SM (nMSSM) or with additional $U(1)'$ gauge symmetries have been considered elsewhere [38], as has the case of explicit CP violation [39].

The NMSSM superpotential is given, in terms of (hatted) superfields, by

$$\mathcal{W} = \lambda \widehat{S} \widehat{H}_u \widehat{H}_d + \frac{\kappa}{3} \widehat{S}^3 + h_t \widehat{Q}_3 \widehat{H}_u \widehat{t}_R^c - h_b \widehat{Q}_3 \widehat{H}_d \widehat{b}_R^c - h_\tau \widehat{L}_3 \widehat{H}_d \widehat{\tau}_R^c, \tag{3.15}$$

in which only the third generation fermions have been included. The first two terms substitute the $\mu \widehat{H}_u \widehat{H}_d$ term in the MSSM superpotential, while the three last terms are the usual generalization of the Yukawa interactions. The soft SUSY breaking terms consist of the scalar mass terms for the Higgs and sfermion scalar fields which, in terms of the fields corresponding to the complex scalar components of the superfields, are given by,

$$\begin{aligned} -\mathcal{L}_{\text{mass}} = {} & m_{H_u}^2 |H_u|^2 + m_{H_d}^2 |H_d|^2 + m_S^2 |S|^2 \\ & + m_{\tilde{Q}_3}^2 \left|\tilde{Q}_3^2\right| + m_{\tilde{t}_R}^2 \left|\tilde{t}_R^2\right| + m_{\tilde{b}_R}^2 \left|\tilde{b}_R^2\right| + m_{\tilde{L}_3}^2 \left|\tilde{L}_3^2\right| + m_{\tilde{\tau}_R}^2 \left|\tilde{\tau}_R^2\right|. \end{aligned} \tag{3.16}$$

The trilinear interactions between the sfermion and Higgs fields are,

$$\begin{aligned} -\mathcal{L}_{\text{tril}} = {} & \lambda A_\lambda H_u H_d S + \frac{1}{3} \kappa A_\kappa S^3 + h_t A_t \tilde{Q}_3 H_u \tilde{t}_R^c - h_b A_b \tilde{Q}_3 H_d \tilde{b}_R^c \\ & - h_\tau A_\tau \tilde{L}_3 H_d \tilde{\tau}_R^c + \text{h.c.} \end{aligned} \tag{3.17}$$

In the unconstrained NMSSM considered here, with non-universal soft terms at the GUT scale, the three SUSY breaking masses squared for H_u, H_d and S appearing in $\mathcal{L}_{\text{mass}}$ can be expressed in terms of their VEVs through the three minimization conditions of the scalar potential. Thus, in

Table 1
Two-loop upper bounds on $\lambda(M_Z)$ for different values of $\kappa(M_Z)$ and $\tan\beta$ in the NMSSM.

$\kappa(M_Z)$	0	0.1	0.2	0.3	0.4	0.5
$\tan\beta = 2$	0.62	0.61	0.60	0.58	0.53	0.42
$\tan\beta = 3$	0.68	0.68	0.66	0.63	0.56	0.45

contrast to the MSSM (where one has only two free parameters at the tree level, generally chosen to be the ratio of Higgs vacuum expectation values, $\tan\beta$, and the mass of the pseudoscalar Higgs boson), the Higgs sector of the NMSSM is described by the six parameters

$$\lambda, \quad \kappa, \quad A_\lambda, \quad A_\kappa, \quad \tan\beta = \langle H_u\rangle/\langle H_d\rangle \quad \text{and} \quad \mu_{\text{eff}} = \lambda\langle S\rangle. \tag{3.18}$$

We follow the sign conventions such that the parameters λ and $\tan\beta$ are positive, while the parameters κ, A_λ, A_κ and μ_{eff} can have both signs.

In addition to these six parameters of the Higgs sector, one needs to specify the soft SUSY breaking mass terms in Eq. (3.16) for the scalars, the trilinear couplings in Eq. (3.17) as well as the gaugino soft SUSY breaking mass parameters to describe the model completely,

$$-\mathcal{L}_{\text{gauginos}} = \frac{1}{2}\left[M_1\tilde{B}\tilde{B} + M_2\sum_{a=1}^{3}\tilde{W}^a\tilde{W}_a + M_3\sum_{a=1}^{8}\tilde{G}^a\tilde{G}_a + \text{h.c.}\right]. \tag{3.19}$$

Clearly, in the limit $\lambda \to 0$ with finite μ_{eff}, the NMSSM turns into the MSSM with a decoupled singlet sector. Whereas the phenomenology of the NMSSM for $\lambda \to 0$ could still differ somewhat from the MSSM in the case where the lightest SUSY particle is the singlino (and hence with the possibility of a long lived next-to-lightest SUSY particle [40]), we will not consider this situation here. In fact we shall be interested exclusively in large values of λ (i.e. $\lambda > 0.5$) in order to increase the tree-level Higgs mass as in Eq. (1.2). For the same reason we shall also focus on moderate values of $\tan\beta$ ($\tan\beta = 2, 3$) that result in the relatively large values of the top quark Yukawa coupling h_t at low energies.

The growth of the Yukawa couplings h_t, λ and κ at the electroweak (EW) scale entails the increase of their values at the Grand Unification scale M_X resulting in the appearance of the Landau pole. Large values of $h_t(M_X)$, $\lambda(M_X)$ and $\kappa(M_X)$ spoil the applicability of perturbation theory at high energies so that the RGEs cannot be used for an adequate description of the evolution of gauge and Yukawa couplings at high scales $Q \sim M_X$. The requirement of validity of perturbation theory up to the Grand Unification scale restricts the interval of variations of Yukawa couplings at the EW scale. In particular, the assumption that perturbative physics continues up to the scale M_X sets an upper limit on the low energy value of $\lambda(M_Z)$ for each fixed set of $\kappa(M_Z)$ and $h_t(M_t)$ (or $\tan\beta$). With decreasing (increasing) $\kappa(M_Z)$ the maximal possible value of $\lambda(M_Z)$, which is consistent with perturbative gauge coupling unification, increases (decreases) for each particular value of $\tan\beta$. In Table 1 we display two-loop upper bounds on $\lambda(M_Z)$ for different values of $\kappa(M_Z)$ and $\tan\beta$ in the NMSSM. As one can see the allowed range for the Yukawa couplings varies when $\tan\beta$ changes. Indeed, for $\tan\beta = 2$ the value of $\lambda(M_Z)$ should be smaller than 0.62 to ensure the validity of perturbation theory up to the scale M_X. At large $\tan\beta$ the allowed range for the Yukawa couplings enlarges. The upper bound on $\lambda(M_Z)$ grows with increasing $\tan\beta$ because the top-quark Yukawa coupling decreases. At large $\tan\beta$ (i.e. $\tan\beta > 4$–5) the upper bound on $\lambda(M_Z)$ approaches the saturation limit where $\lambda_{\max} \simeq 0.72$.

The renormalisation group (RG) flow of the Yukawa couplings depends rather strongly on the values of the gauge couplings at the intermediate scales. To demonstrate this we examine

Table 2
Two-loop upper bounds on $\lambda(M_Z)$ for different values of $\kappa(M_Z)$ and $\tan\beta$ within the NMSSM supplemented by three $SU(5)$ $(5+\bar{5})$-plets. The masses of all extra exotic states are set to be equal to 300 GeV.

$\kappa(M_Z)$	0	0.1	0.2	0.25	0.3	0.4	0.5
$\tan\beta = 2$	0.72	0.72	0.7	0.67	0.65	0.57	0.45
$\tan\beta = 3$	0.76	0.75	0.73	0.70	0.67	0.59	0.47

Table 3
Two-loop upper bounds on $\lambda(M_Z)$ for different values of $\kappa(M_Z)$ and $\tan\beta$ within the NMSSM supplemented by three $SU(5)$ $(5+\bar{5})$-plets. The masses of all extra exotic states are set to be equal to 1 TeV.

$\kappa(M_Z)$	0	0.1	0.2	0.25	0.3	0.4	0.5
$\tan\beta = 2$	0.71	0.7	0.68	0.66	0.64	0.56	0.45
$\tan\beta = 3$	0.74	0.74	0.72	0.69	0.67	0.59	0.46

the RG flow of gauge and Yukawa couplings within the SUSY model that contains three extra $SU(5)$ $(5+\bar{5})$-plets that survive to low energies and can form three 10-plets in the SUSY-GUT model based on the $SO(10)$ gauge group. In this SUSY model the strong gauge coupling has a zero one-loop beta function whereas at two-loop level the coupling has a mild growth as the renormalisation scale increases. Since extra states form complete $SU(5)$ multiplets the high-energy scale where the unification of the gauge couplings takes place remains almost the same as in the MSSM. At the same time extra multiplets of matter change the running of the gauge couplings so that their values at the intermediate scale rise substantially. In fact the two-loop beta functions of the SM gauge couplings are quite close to their saturation limits when these couplings blow up at the GUT scale. Further enlargement of the particle content can lead to the appearance of the Landau pole during the evolution of the gauge couplings from M_Z to M_X. Because the beta functions are so close to the saturation limits the RG flow of the gauge couplings (i.e. their values at the intermediate scale) also depends on the masses of the extra exotic states. Since $g_i(Q)$ occurs in the right-hand side of the RGEs for the Yukawa couplings with negative sign the growth of the gauge couplings prevents the appearance of the Landau pole in the evolution of these couplings. It means that for each value of $h_t(M_t)$ (or $\tan\beta$) and $\kappa(M_Z)$ the upper limit on $\lambda(M_Z)$ increases as compared with the NMSSM. The two-loop upper bounds on $\lambda(M_Z)$ for different values of $\kappa(M_Z)$ and $\tan\beta$ in the NMSSM supplemented by three $SO(10)$ 10-plets, or equivalently three $SU(5)$ $(5+\bar{5})$-plets are displayed in Table 2 for the case that the masses of all extra exotic states are set to be equal to 300 GeV and in Table 3 in case they are set to be equal to 1 TeV. The two-loop RGEs used to obtain these results are given in Appendix A. Because the RG flow of the gauge couplings depends on the masses of extra exotic states the upper bounds on $\lambda(M_Z)$ presented in Tables 2 and 3 are slightly different. The restrictions on $\lambda(M_Z)$ obtained in this section are useful for the phenomenological analysis which we are going to consider next.

4. Constraints from Higgs boson searches, SUSY particle searches and dark matter

Our scenarios are subject to constraints on the Higgs boson masses from the direct searches at LEP, Tevatron and the LHC. Also the SUSY particle masses have to be compatible with the limits given by the experiments. Finally, the currently measured value of the relic density shall be reproduced. Further constraints arise from the low-energy observables.

4.1. Higgs boson searches

We start by discussing the constraints which arise from the LHC search for the Higgs boson. At the LHC, the most relevant Higgs boson production channels for neutral (N)MSSM Higgs bosons are given by gluon fusion, gauge boson fusion, Higgs-strahlung and associated production with a heavy quark pair. The two main mechanisms for charged Higgs boson production are top quark decay and associated production with a heavy quark pair. For reviews, see [8,41,42]. As in our scenarios the charged Higgs boson mass is larger than 450 GeV and hence well beyond the sensitivity of Tevatron and current LHC searches, we will discuss in the following only neutral Higgs boson production.

4.1.1. Gluon fusion

In the SM and in SUSY extensions, such as the (N)MSSM, for low values of $\tan\beta$, the most important production channel is given by gluon fusion [43]. In the NMSSM we have

$$gg \to H_i \quad \text{and} \quad gg \to A_j, \quad i = 1,2,3,\ j = 1,2. \tag{4.20}$$

Since this is the dominant Higgs production mechanism for a 125 GeV Higgs boson at the LHC, we find it convenient to define for later use the ratio of the gluon fusion production cross-section for the Higgs boson H_i in the NMSSM to the gluon fusion production cross-section for a SM Higgs boson H^{SM} of same mass as H_i,

$$R_{\sigma_{gg}}(H_i) \equiv \frac{\sigma(gg \to H_i)}{\sigma(gg \to H^{SM})}. \tag{4.21}$$

Gluon fusion is mediated by heavy quark loops in the SM and additionally by heavy squark loops in the (N)MSSM. It is subject to important higher-order QCD corrections. For the SM, they have been calculated at next-to-leading order (NLO) [44] including the full mass dependence of the loop particles and in the heavy top quark limit, and up to next-to-next-to-leading order (NNLO) in the heavy top quark limit [45]. The cross-section has been improved by soft-gluon resummation at next-to-next-to-leading logarithmic (NNLL) accuracy [46]. Top quark mass effects on the NNLO loop corrections have been studied in [47], and the EW corrections have been provided in [48]. In the MSSM, the QCD corrections have been calculated up to NLO [44]. The QCD corrections to squark loops have been first considered in [49] and at full NLO SUSY-QCD in the heavy mass limit in [50]. The (s)bottom quark contributions at NLO SUSY-QCD have been taken into account through an asymptotic expansion in the SUSY particle masses [51]. For squark masses below ∼400 GeV, mass effects play a role and can alter the cross-section by up to 15% compared to the heavy mass limit as has been shown for the QCD corrections to the squark loops in [52,53]. The SUSY QCD corrections including the full mass dependence of all loop particles have been provided by [54]. The mass effects turn out to be sizeable. The NNLO SUSY-QCD corrections from the (s)top quark sector to the matching coefficient determining the effective Higgs gluon vertex have been calculated in [55].

The gluon fusion cross-section has been implemented in the Fortran code `HIGLU` [56] up to NNLO QCD. While at NLO the full mass dependence of the loop particles is taken into account the NNLO corrections are obtained in an effective theory approach. In the MSSM the full squark mass dependence in the NLO QCD corrections to the squark loops is included [53]. Note, however, that in the MSSM at NNLO the mismatch in the QCD corrections to the effective vertex is not taken into account, neither the SUSY QCD corrections to the effective vertex. The former should be only a minor effect, though, as the dominant effect of the QCD higher-order

corrections stems from the gluon radiation. Furthermore, the EW corrections to the SM can be obtained with HIGLU. In order to check if our scenario is compatible with the recent LHC results, we need the cross-section of a SM-like Higgs boson of 124 to 126 GeV. The experiments include in their analyses the NNLO QCD (CMS also the NNLL QCD and NLO EW) corrections [1,2] to the gluon fusion cross-section as provided by the Higgs Cross-Section Working Group [42]. For SUSY, however, the EW corrections are not available. In order to be consistent, we therefore compare in the following the NMSSM cross-section to the SM cross-section at NNLO QCD. As the QCD corrections are not affected by modifications of the Higgs couplings to the (s)quarks, the NMSSM cross-section can be obtained with the program HIGLU by multiplying the MSSM Higgs couplings with the corresponding modification factor of the NMSSM Higgs couplings to the (s)quarks with respect to the MSSM case. We have implemented these coupling modification factors in the most recent HIGLU version 3.11.

4.1.2. W/Z-boson fusion

Gauge boson fusion [57] plays an important role for light CP-even Higgs boson production in the SM limit,[2]

$$qq \to qq + W^*W^*/Z^*Z^* \to qqH_i, \quad i = 1, 2, 3. \tag{4.22}$$

Otherwise the (N)MSSM cross-section is suppressed with respect to the SM case by mixing angles entering the Higgs couplings to the gauge bosons. The NLO QCD corrections are of $\mathcal{O}(10\%)$ of the total cross-section [58,59]. The full EW and QCD corrections to the SM are $\mathcal{O}(5\%)$ [60]. The NNLO QCD effects on the cross-section amount to $\sim$2% [61]. The SUSY QCD and SUSY EW corrections are small [62,63]. Once again, as QCD corrections are not affected by the Higgs couplings to the gauge bosons, the QCD corrected NMSSM gauge boson fusion production cross-sections can be derived from the QCD corrected SM cross-section by simply applying the modification factor of the respective NMSSM Higgs coupling to the gauge bosons with respect to the SM coupling,

$$\sigma_{QCD}^{NMSSM}(qqH_i) = \left(\frac{g_{VVH_i}}{g_{VVH^{SM}}}\right)^2 \sigma_{QCD}^{SM}(qqH^{SM}), \quad V = W, Z, \tag{4.23}$$

where g denotes the coupling. The EW corrections, however, cannot be taken over. We have obtained the SM production cross-section at NLO QCD from the program VV2H [64]. While the experiments use the SM cross-section at NNLO QCD (CMS also at NLO EW), the effects of these additional corrections in the SM limit, where we compare our NMSSM Higgs cross-section to the SM case, are small.

4.1.3. Higgs-strahlung

The CP-even Higgs bosons can also be produced in Higgs-strahlung [65],

$$qq \to VH_i, \quad V = W, Z, \ i = 1, 2, 3, \tag{4.24}$$

with the NMSSM cross-section always being suppressed by mixing angles compared to the SM cross-section. The QCD corrections apply both to the SM and (N)MSSM case. While the NLO QCD corrections increase the cross-section by $\mathcal{O}(30\%)$ [59,66] the NNLO QCD corrections are

[2] The quark q stands for a generic quark flavour, which is different for the two quarks in case of W-boson fusion. The same notation is applied below in Higgs-strahlung.

small [67]. The full EW corrections are only known for the SM and decrease the cross-section by $\mathcal{O}(5\text{–}10\%)$ [68]. The SUSY-QCD corrections amount to less than a few percent [62]. The NLO QCD SM Higgs-strahlung cross-section has been obtained with the program V2HV [64]. The NMSSM Higgs production cross-sections can be derived from it by applying the Higgs coupling modification factors,

$$\sigma_{QCD}^{NMSSM}(VH_i) = \left(\frac{g_{VVH_i}}{g_{VVH^{SM}}}\right)^2 \sigma_{QCD}^{SM}\left(VH^{SM}\right), \quad V = W, Z. \tag{4.25}$$

The experiments use the QCD corrected cross-section up to NNLO (CMS also including the NLO EW corrections). While we neglect the NNLO and EW corrections, we do not expect this to influence significantly the total cross-section composed of all production channels, in view of the small size of the total Higgs-strahlung cross-section itself.

4.1.4. Associated production with heavy quarks

Associated production of (N)MSSM Higgs bosons with top quarks [69] only plays a role for the light scalar Higgs particle and small values of $\tan\beta$ due to the suppression of the Higgs couplings to top quarks $\sim 1/\tan\beta$. While associated production with bottom quarks [69,70] does not play a role in the SM, in the (N)MSSM this cross-section becomes important for large values of $\tan\beta$ and can exceed the gluon fusion cross-section. As our scenarios include small values of $\tan\beta$ we will not further discuss this cross-section here. The values for the SM $t\bar{t}H$ cross-section including NLO QCD corrections [71], which are of moderate size, can be obtained from the Higgs Cross Section Working Group homepage [72]. From these we derived the NMSSM cross-section values by replacing the SM Yukawa couplings with the NMSSM Yukawa couplings,

$$\sigma_{QCD}^{NMSSM}(t\bar{t}H_i) = \left(\frac{g_{t\bar{t}H_i}}{g_{t\bar{t}H^{SM}}}\right)^2 \sigma_{QCD}^{SM}\left(t\bar{t}H^{SM}\right). \tag{4.26}$$

The NLO SUSY QCD corrections, which have not been taken into account by the experiments, are of moderate size [73].

4.2. Constraints from the LHC searches

Recent results presented by the ATLAS [1] and the CMS [2] Collaborations seem to indicate a Higgs boson of mass of 126 and 124 GeV, respectively. Based on the dataset corresponding to an integrated luminosity of up to 4.9 fb^{-1} collected at $\sqrt{s} = 7$ TeV, an excess of events is observed by the ATLAS experiment for a Higgs boson mass hypothesis close to $M_H = 126$ GeV with a maximum local significance of 3.6σ above the expected SM background. The three most sensitive channels in this mass range are given by $H \to \gamma\gamma$, $H \to ZZ^{(*)} \to l^+l^-l^+l^-$ and $H \to WW^{(*)} \to l^+\nu l^-\bar{\nu}$. The CMS Collaboration presented results of SM Higgs boson searches in the mass range 100–600 GeV in 5 decay modes, $H \to \gamma\gamma, bb, \tau\tau, WW$ and ZZ. The data correspond to an integrated luminosity of up to 4.7 fb^{-1} at $\sqrt{s} = 7$ TeV. A modest excess of events is observed for Higgs boson mass hypotheses towards the low end of the investigated Higgs mass range. The maximum local significance amounts to 2.6σ for a Higgs boson mass hypothesis of $M_H = 124$ GeV. For our NMSSM benchmark scenarios presented below to be consistent with these LHC results we demand the production cross-section of the SM-like NMSSM Higgs boson with mass 124 GeV to 126 GeV (depending on the scenario) to be compatible within 20% with the production cross-section of a SM Higgs boson of same mass. The 20% are driven by the theoretical uncertainty on the inclusive Higgs production cross-section given by the sum of the

most relevant production channels at low values of $\tan\beta$, i.e. gluon fusion, weak boson fusion, Higgs-strahlung and $t\bar{t}$ Higgs production. The theoretical error is largest for the gluon fusion cross-section with 10–15% at these Higgs mass values and $\sqrt{s} = 7$ TeV [42], and which contributes dominantly to the inclusive production. We do not consider any experimental error since this is beyond our scope.

For simplicity, and since these search channels are common to both experimental analyses, we consider the Higgs decays into $\gamma\gamma$, $ZZ \to 4l$ and $WW \to 2l2\nu$. In order to get an estimate of how closely the NMSSM Higgs resembles the SM Higgs in LHC searches in these channels we define the ratios of branching ratios into massive gauge boson final states VV, where $V = W, Z$,[3] and into $\gamma\gamma$, respectively, for an NMSSM Higgs boson H_i and the SM Higgs boson H^{SM} of same mass,

$$R_{VV}(H_i) \equiv \frac{\mathrm{BR}(H_i \to VV)}{\mathrm{BR}(H^{SM} \to VV)} \quad \text{and} \quad R_{\gamma\gamma}(H_i) \equiv \frac{\mathrm{BR}(H_i \to \gamma\gamma)}{\mathrm{BR}(H^{SM} \to \gamma\gamma)}. \tag{4.27}$$

We also define analogously $R_{\Gamma_{tot}}$ for the total widths,

$$R_{\Gamma_{tot}}(H_i) \equiv \frac{\Gamma_{tot}(H_i)}{\Gamma_{tot}(H^{SM})}, \tag{4.28}$$

and $R_{b\bar{b}}(H_i)$ for the decay into $b\bar{b}$. Although this final state is not useful for LHC searches, it is interesting to show as in this mass range and for small values of $\tan\beta$ the decay into $b\bar{b}$ contributes dominantly to the total width. Depending on of how much H_d component is in the mass eigenstate H_i it is enhanced or suppressed compared to the SM. This directly influences the total width and hence the branching ratios of the other final states.

For a crude estimate of the total Higgs cross-section at the LHC, we can combine these channels in quadrature in contrast to the experiments which do a sophisticated statistical combination of the various search channels, which is, however, beyond the scope of our theoretical analysis. Our results should therefore only be regarded as a rough estimate which is indicative enough, however, at the present status of the experimental research, to exclude or not exclude a benchmark scenario. We hence demand for a scenario to be valid that one of the NMSSM Higgs bosons H_i satisfies

$$0.8\sigma_{tot}\big(H^{SM}\big) \leqslant \sigma_{tot}(H_i) \leqslant 1.2\sigma_{tot}\big(H^{SM}\big), \tag{4.29}$$

where

$$\begin{aligned}\sigma_{tot}(H) = \sigma_{incl}(H)\big\{&\mathrm{BR}^2(H \to \gamma\gamma) + 16\mathrm{BR}^2(H \to ZZ)\mathrm{BR}^2(Z \to ll)\mathrm{BR}^2(Z \to ll) \\ &+ 16\mathrm{BR}^2(H \to WW)\mathrm{BR}^2(W \to l\nu)\mathrm{BR}^2(W \to l\nu)\big\}^{1/2}.\end{aligned} \tag{4.30}$$

The inclusive cross-section σ_{incl} is composed of gluon fusion, vector boson fusion, Higgs-strahlung and associated production with $t\bar{t}$,

$$\sigma_{incl}(H) = \sigma(gg \to H) + \sigma(Hqq) + \sigma(WH) + \sigma(ZH) + \sigma(t\bar{t}H), \tag{4.31}$$

with $H = H_i, H^{SM}$, respectively, subject to the constraint $M_{H^{SM}} = M_{H_i} = 124$–$126$ GeV, depending on the scenario under consideration. It is dominated by the gluon fusion cross-section.

[3] The ratio is the same for WW and ZZ final states, respectively, as the NMSSM coupling to WW and ZZ is suppressed by the same factor compared to the SM.

The factors 16 in Eq. (4.30) arise from the sum of the four possible lepton final states in the decays of the Z- and W-boson pairs, respectively. (We neglect interference effects.) For the gauge boson branching ratios we chose the values given by the Particle Data Group [74],

$$\mathrm{BR}(Z \to ll) = 0.0366, \qquad \mathrm{BR}(W \to l\nu) = 0.1080. \tag{4.32}$$

It is useful to define

$$R_{\sigma_{tot}}(H_i) = \frac{\sigma_{tot}(H_i)}{\sigma_{tot}(H^{SM})}, \tag{4.33}$$

in order to provide a measure of how closely the NMSSM Higgs resembles the SM Higgs in the most important current LHC search channels. The total cross-section is dominated by the WW-boson final state due to the large branching ratio. As we will see below, in the NMSSM the branching ratio into $\gamma\gamma$ can be enhanced for certain parameter configurations compared to the SM. To illustrate this effect, we therefore also calculate separately the ratios of the expected number of events in the NMSSM compared to the SM for the $\gamma\gamma$ final state and for the VV ($V = W, Z$) final state, which is the same for $V = W$ or Z. They are given by

$$R_{\sigma_{incl}}(H_i)R_{\gamma\gamma}(H_i) \quad \text{and} \quad R_{\sigma_{incl}}(H_i)R_{VV}(H_i), \tag{4.34}$$

where $R_{\sigma_{incl}}(H_i) = \sigma_{incl}(H_i)/\sigma_{incl}(H^{SM})$.

4.3. NMSSM spectrum and NMSSM Higgs boson branching ratios

The SUSY particle and NMSSM Higgs boson masses and branching ratios are calculated with the program package `NMSSMTools` [21,35,36]. As for the NMSSM Higgs boson masses, the leading one-loop contributions due to heavy (s)quark loops calculated in the effective potential approach [75], the one-loop contributions due to chargino, neutralino and scalar loops in leading logarithmic order in Ref. [76] and the leading logarithmic two-loop terms of $\mathcal{O}(\alpha_t\alpha_s)$ and $\mathcal{O}(\alpha_t^2)$, taken over from the MSSM results, have been implemented in `NMSSMTools`. The full one-loop contributions have been computed in the $\overline{\mathrm{DR}}$ renormalisation scheme [77,78] and also in a mixed on-shell (OS) and $\overline{\mathrm{DR}}$ scheme as well as in a pure OS scheme [79]. Furthermore, the $\mathcal{O}(\alpha_t\alpha_s + \alpha_b\alpha_s)$ corrections have been provided in the approximation of zero external momentum [77]. The corrections provided by Ref. [77] have been implemented in `NMSSMTools` as well.

The calculation of the NMSSM Higgs boson decay widths and branching ratios within `NMSSMTools` is performed by the Fortran code `NMHDECAY` [21,35] which uses to some extent parts of the Fortran code `HDECAY` [80,81] that calculates SM and MSSM Higgs boson partial widths and branching ratios. The calculation of the SUSY particle branching ratios on the other hand with the Fortran code `NMSDECAY` [82] is based on a generalisation of the Fortran code `SDECAY` [81,83] to the NMSSM case. `NMSSMTools` provides the output for the complete NMSSM particle spectrum and mixing angles and for the decays in the SUSY Les Houches format [84]. The latter can be read in by our own Fortran version for NMSSM Higgs boson decays based on an extension of the latest `HDECAY` version. It reads in the particle spectrum and mixing angles created with `NMSSMTools`, calculates internally the NMSSM Higgs boson couplings and uses them to calculate the Higgs decay widths and branching ratios. The results for the branching ratios from `NMSSMTools` and from our own program agree reasonably well and the differences in the total cross-section equation (4.30), obtained with the results from the two programs, due to deviations in the branching ratios are in the percent range.

4.4. Constraints from dark matter, low energy observables, LEP and Tevatron

Based on an interface between NMHDECAY and micrOMEGAs [85] the relic abundance of the NMSSM dark matter candidate $\tilde{\chi}_1^0$ can be evaluated using NMSSMTools. As an independent check, we also used the stand alone code micrOMEGAs to calculate the relic density. All the relevant cross-sections for the lightest neutralino annihilation and co-annihilation are computed. The density evolution equation is numerically solved and the relic density of $\tilde{\chi}_1^0$ is calculated. The differences in the result for the relic density calculated with both tools are negligible. The results are compared with the "WMAP" constraint $0.094 \lesssim \Omega_{\rm CDM} h^2 \lesssim 0.136$ at the 2σ level [86].

When the spectrum and the couplings of the Higgs and SUSY particles are computed with NMSSMTools, constraints from low-energy observables as well as available Tevatron and LEP constraints are checked. The results of the four LEP collaborations, combined by the LEP Higgs Working Group, are included [87]. More specifically, the following experimental constraints are taken into account:

(i) The masses of the neutralinos as well as their couplings to the Z^0-boson are compared with the LEP constraints from direct searches and from the invisible Z^0-boson width.
(ii) Direct bounds from LEP and Tevatron on the masses of the charged particles ($h^\pm$, $\chi^\pm$, $\tilde{q}$, $\tilde{l}$) and the gluino are taken into account.
(iii) Constraints on the Higgs production rates from all channels studied at LEP. These include in particular ZH_i production, H_i being any of the CP-even Higgs particles, with all possible two body decay modes of H_i (into b quarks, τ leptons, jets, photons or invisible), and all possible decay modes of H_i of the form $H_i \to A_j A_j$, A_j being any of the CP-odd Higgs particles, with all possible combinations of A_j decays into b quarks, c quarks, τ leptons and jets. Also considered is the associated production mode $e^+e^- \to H_i A_j$ with, possibly, $H_i \to A_j A_j$. (In practice, for our purposes, only combinations of $i = 1, 2$ with $j = 1$ are phenomenologically relevant.)
(iv) Experimental constraints from B physics [88] such as the branching ratios of the rare decays $\mathrm{BR}(B \to X_s\gamma)$, $\mathrm{BR}(B_s \to \mu^+\mu^-)$ and $\mathrm{BR}(B^+ \to \tau^+\nu_\tau)$ and the mass differences ΔM_s and ΔM_d, are also implemented; compatibility of each point in parameter space with the current experimental bounds is required at the two sigma level.

4.5. Constraints on SUSY particle masses from the LHC

The ATLAS [89] and CMS [90] searches in final states with jets and missing transverse energy E_T^{miss}, with large jet multiplicities and E_T^{miss}, with heavy flavour jets and E_T^{miss} within simplified models and mSUGRA/constrained MSSM (CMSSM) models set limits on the masses of gluino and squark masses. Further constraints are obtained from searches in final states with leptons and taus [91]. The precise exclusion limits depend on the investigated final state, the value of the neutralino and/or chargino masses and the considered model. Light gluino (below about 600 GeV) and squark masses (below about 700 GeV) are excluded. The limits cannot be applied, however, to the third generation squarks in a model-independent way. Recent analyses scanning over the physical stop and sbottom masses and translating the limits to the third generation squark sector have shown that the sbottom and stop masses can still be as light as $\sim$ 200–300 GeV depending on the details of the spectrum [92]. Especially scenarios, where the lightest stop is the next-to-lightest SUSY particle (NLSP) and nearly degenerate with the lightest neutralino assumed to be

the lightest SUSY particle (LSP), are challenging for the experiments. Such scenarios can be consistent with Dark Matter constraints due to possible co-annihilation [93]. If the $\tilde{t}_1 - \tilde{\chi}_1^0$ mass difference is small enough, the flavour-changing neutral current decay $\tilde{t}_1 \to c\tilde{\chi}_1^0$ [94] is dominating and can compete with the four-body decay into the LSP, a b quark and a fermion pair [95]. Limits have been placed by the Tevatron searches [96] and depending on the neutralino mass still allow for very light stops down to 100 GeV. The authors of Ref. [97] found that translating the LHC limits to stop searches in the co-annihilation scenario [98][4] allows for stops lighter than ∼400 GeV down to 160 GeV. We are not aware, however, of any dedicated LHC analysis which excludes very light stops.

5. The benchmark points

In this section we present benchmark points for the NMSSM with a SM-like Higgs boson near 125 GeV. The Higgs sector of the NMSSM has a rich parameter space including $\lambda, \kappa, A_\lambda, A_\kappa, \tan\beta$ and the effective μ parameter. According to the SLHA format [84], these parameters are understood as running $\overline{\text{DR}}$ parameters taken at the SUSY scale $\tilde{M} = 1$ TeV while $\tan\beta$ is taken at the scale of the Z-boson mass, M_Z. In order not to violate tree-level naturalness we set $\mu_{\text{eff}} \leqslant 200$ GeV for all the considered points. The Higgs sector is strongly influenced by the stop sector via radiative corrections where we further need to specify the soft SUSY breaking masses $M_{\tilde{Q}_3}, M_{\tilde{t}_R}$ and the mixing parameter X_t defined in Eq. (2.7). The main advantage of the NMSSM over the MSSM, regarding a SM-like Higgs boson near 125 GeV, is that the stop masses are allowed to be much lighter, making the NMSSM much more technically natural than the MSSM. Thus all of the benchmarks discussed here will involve relatively light stops, with masses well below 1 TeV. We choose low values of $\tan\beta = 2, 3$ in order to maximise the tree-level contribution to the Higgs boson mass, allowing the stops to be lighter. For very light stops, in order not to be in conflict with the present exclusion limits, the difference between the $\tilde{t}_1$ and $\tilde{\chi}_1^0$ masses should be less than ∼ 20–30 GeV to be in the co-annihilation region. By choosing the right-handed stop to be the lightest top squark the sbottoms are still heavy enough to fulfill the LHC limits of about 300 GeV [100] also in this case. On the other hand, the remaining squarks and sleptons may be heavier without affecting fine-tuning. In order to satisfy in particular the LHC search limits for the squarks of the first two generations, we set all their masses to be close to 1 TeV and, for simplicity, also those of the sleptons. To be precise, for the first and second squark and slepton families and for the stau sector we always take the soft SUSY breaking masses and trilinear couplings to be 1 TeV, and furthermore, the right-handed soft SUSY breaking mass and trilinear coupling of the sbottom sector is set to 1 TeV, i.e. ($U \equiv u, c$, $D \equiv d, s$, $E \equiv e, \mu, \tau$)

$$\begin{aligned} &M_{\tilde{U}_R} = M_{\tilde{D}_R} = M_{\tilde{b}_R} = M_{\tilde{Q}_{1,2}} = M_{\tilde{E}_R} = M_{\tilde{L}_{1,2,3}} = 1 \text{ TeV}, \\ &A_U = A_D = A_b = A_E = 1 \text{ TeV}. \end{aligned} \tag{5.35}$$

This results in physical masses of ∼1 TeV for the first and second family squarks and sleptons as well as the heavier sbottom. These masses can readily be increased without affecting the properties of the quoted benchmark points appreciably. The gaugino mass parameters have been set such that they fulfill roughly GUT relations. Special attention has been paid, however, not to choose the gluino mass too heavy in order to avoid fine-tuning. Before discussing the benchmark points, a few technical preliminaries are in order. The masses for the Higgs bosons and SUSY

[4] For stop searches in scenarios with light gravitinos see [99].

Table 4
Branching ratios into $\gamma\gamma$, ZZ, WW, $b\bar{b}$ and total width of a SM Higgs boson of mass between 123.5 and 126.5 GeV.

M_H [GeV]	BR($H \to \gamma\gamma$)	BR($H \to ZZ$)	BR($H \to WW$)	BR($H \to b\bar{b}$)	Γ_{tot} [GeV]
123.5	$2.334 \cdot 10^{-3}$	0.018	0.174	0.616	$3.773 \cdot 10^{-3}$
123.6	$2.335 \cdot 10^{-3}$	0.018	0.175	0.615	$3.784 \cdot 10^{-3}$
123.7	$2.336 \cdot 10^{-3}$	0.019	0.177	0.613	$3.795 \cdot 10^{-3}$
123.8	$2.337 \cdot 10^{-3}$	0.019	0.179	0.612	$3.807 \cdot 10^{-3}$
124	$2.338 \cdot 10^{-3}$	0.019	0.182	0.609	$3.830 \cdot 10^{-3}$
124.5	$2.342 \cdot 10^{-3}$	0.020	0.189	0.601	$3.890 \cdot 10^{-3}$
124.6	$2.343 \cdot 10^{-3}$	0.021	0.191	0.600	$3.903 \cdot 10^{-3}$
125	$2.345 \cdot 10^{-3}$	0.021	0.197	0.594	$3.953 \cdot 10^{-3}$
125.8	$2.347 \cdot 10^{-3}$	0.023	0.210	0.581	$4.058 \cdot 10^{-3}$
126	$2.348 \cdot 10^{-3}$	0.024	0.213	0.578	$4.085 \cdot 10^{-3}$
126.2	$2.348 \cdot 10^{-3}$	0.024	0.217	0.575	$4.113 \cdot 10^{-3}$
126.5	$2.348 \cdot 10^{-3}$	0.025	0.222	0.570	$4.155 \cdot 10^{-3}$

particles have been obtained using NMSSMTools. In the presentation of our benchmark scenarios, for the SM-like Higgs boson we furthermore include the ratios of the branching ratios, *cf.* Eq. (4.27), into $\gamma\gamma$, $b\bar{b}$ and VV ($V = Z, W$) as well as the ratio of the total widths, Eq. (4.28), for the NMSSM and SM Higgs boson having the same mass. The NMSSM branching ratios and total width have been obtained with NMSSMTools and cross-checked against a private code whereas the SM values have been calculated with HDECAY. The latter are shown separately in Table 4 for a SM Higgs boson with the mass values corresponding to the various masses of the SM-like NMSSM Higgs boson in our benchmark scenarios. The NMSSM values can be obtained by multiplication with the corresponding ratios presented in the benchmark tables, although it is mainly their relative values, compared to the SM, that concern us here. Note that HDECAY includes the double off-shell decays into massive vector bosons, whereas NMSSMTools does not. We therefore turned off the double off-shell decays also in HDECAY. This explains why the SM values given in Table 4 differ from the values given on the website of the Higgs Cross Section Working Group [72]. There are further differences between the two programs in the calculation of the various partial widths. Thus HDECAY includes the full NNNLO corrections to the top loops in the decay into gluons. Also it uses slightly different running bottom and charm quark masses. Taking all these effects into account we estimate the theoretical error on the ratios of branching ratios, which are calculated with these two different programs, to be of the order of 5%. This should be kept in mind when discussing the benchmark scenarios.

As mentioned above, in order to be compatible with the recent LHC results for the Higgs boson search we demand the total cross-section as defined in Eq. (4.30) to be within 20% equal to the corresponding SM cross-section. We therefore include in our tables for the benchmark points the ratio $R_{\sigma_{tot}}$, Eq. (4.33), of the NMSSM and SM total cross-section for $\sqrt{s} = 7$ TeV and for completeness also the ratio $R_{\sigma_{gg}}$, Eq. (4.21), of the NMSSM and SM gluon fusion cross-sections since gluon fusion is the dominant contribution to inclusive Higgs production for low values of $\tan\beta$ at the LHC. The latter has been obtained with the Fortran code HIGLU at NNLO QCD and includes the squark loop contributions. Note, that we did not include electroweak corrections. Furthermore, we explicitly verified that $R_{\sigma_{tot}}$ is practically the same using NLO or NNLO QCD gluon fusion cross-sections. The values of the gluon fusion cross-section and of the total cross-section at NLO and NNLO QCD are shown separately for the SM in Table 5. However, the ratios for the cross-sections which we present in the tables, $R_{\sigma_{gg}}$, $R_{\sigma_{tot}}$, are for the case of gluon fusion production at NNLO QCD. With the total cross-section being dominated by the WW-boson final

Table 5
The NLO and NNLO cross-sections for gluon fusion into a SM Higgs boson and the total cross-section as defined in Eq. (4.30) including an NLO and NNLO gluon fusion cross-section, respectively, for various values of the SM Higgs boson mass.

M_H [GeV]	σ_{gg}^{NLO} [pb]	σ_{gg}^{NNLO} [pb]	σ_{tot}^{NLO} [pb]	σ_{tot}^{NNLO} [pb]
123.5	13.08	15.44	0.134	0.155
123.6	13.06	15.41	0.135	0.156
123.7	13.04	15.39	0.136	0.157
123.8	13.02	15.36	0.137	0.158
124	12.97	15.31	0.138	0.160
124.5	12.87	15.18	0.143	0.165
124.6	12.85	15.15	0.144	0.166
125	12.76	15.05	0.147	0.170
125.8	12.59	14.85	0.154	0.178
126	12.55	14.80	0.156	0.180
126.2	12.51	14.75	0.158	0.182
126.5	12.45	14.68	0.161	0.185

state, in order to illustrate interesting effects in the NMSSM branching ratios compared to the SM ones, for the SM-like Higgs boson we also give separately the ratios of the expected number of events in the $\gamma\gamma$ and VV ($V = W, Z$) final states as given by Eq. (4.34).

All our presented scenarios fulfill the cross-section constraint, Eq. (4.29), and are hence compatible with the LHC searches, keeping in mind though that as theorists we can do only a rough estimate here. Furthermore, they fulfill the constraints from low-energy parameters as specified in Section 4 and are compatible with the measurement of the relic density. In principle they could also account for the 3σ deviation of the muon anomalous magnetic momentum from the SM if we were to lower the smuon mass, but for clarity we have taken all first and second family squark and slepton masses to be close to 1 TeV, as discussed above.

We consider four different sets of NMSSM benchmark points as follows:

- **NMSSM with lightest Higgs being SM-like near 125 GeV**
  This is achieved with $\lambda = 0.57$–0.64 and $\kappa = 0.18$–0.25 such that λ does not blow up below the GUT scale in the usual NMSSM with no extra matter as in Table 1. This set of benchmarks is displayed in Table 6.
- **NMSSM with second lightest Higgs being SM-like near 125 GeV**
  This is achieved with $\lambda = 0.55$–0.67 and $\kappa = 0.10$–0.31 such that λ does not blow up below the GUT scale in the usual NMSSM with no extra matter as in Table 1. This set of benchmarks is displayed in Table 7.
- **NMSSM-with-extra-matter and second Higgs being SM-like near 125 GeV**
  This is achieved with $\lambda = 0.68$–0.69 and $\kappa = 0.06$–0.20 such that λ does not blow up below the GUT scale in the NMSSM supplemented by three $SO(10)$ 10-plets as in Table 3. The slightly larger value of λ here allows extra matter to be at or above the TeV scale. This set of benchmarks is displayed in Table 8.
- **NMSSM-with-extra-matter and lightest Higgs being SM-like near 125 GeV**
  This is achieved with $\lambda = 0.7$ and $\kappa = 0.20$–0.25 such that λ does not blow up below the GUT scale in the NMSSM supplemented by three $SO(10)$ 10-plets as in Table 2. The larger values of λ and κ here requires the extra matter to be close to the electroweak scale. This set of benchmarks is displayed in Table 9.

Note that the input values for λ and κ are taken at the scale 1 TeV. Their corresponding values at M_Z are lower so that we are well within the limits given in Tables 1–3. Within each set we have selected three benchmark points which are chosen to illustrate key features of the NMSSM Higgs boson which could be used to resolve it from the SM Higgs state in future LHC searches. This makes 12 benchmark points in total which we label as NMP1 to NMP12. In the following we discuss the key features of each of the points in detail under the above four headings. Since we focus on large values of $\lambda \gtrsim 0.55$ and moderate values of $\tan\beta = 2, 3$ the requirement of the validity of perturbation theory up to the GUT scale constrains the low energy value of the coupling to be $\kappa \lesssim 0.3$. As a result the heaviest CP-even, CP-odd and charged Higgs states are almost degenerate and substantially heavier than the two lightest Higgs scalars and the lightest Higgs pseudoscalar for all the benchmark points, as discussed in [14]. Also note that all the benchmark points satisfy the WMAP relic abundance. Depending on the decomposition of the lightest neutralino and its mass value the main annihilation channels are $\tilde{\chi}_1^0\tilde{\chi}_1^0 \to W^+W^-$ or $\tilde{\chi}_1^0\tilde{\chi}_1^0 \to q\bar{q}$ $(q = b, s, d, c, u)$. For very light stops $\tilde{t}_1$ with mass near the $\tilde{\chi}_1^0$ mass, as in the benchmark point NMP8, the dominant channel is the coannihilation channel, $\tilde{t}_1\tilde{\chi}_1^0 \to W^+b$.

5.1. NMSSM with lightest Higgs being SM-like

Table 6 shows three points NMP1, NMP2, NMP3 which satisfy NMSSM perturbativity up to the GUT scale and lead to the SM-like Higgs boson always being the lightest one H_1 near 125 GeV. The mass of the second lightest Higgs boson H_2 ranges between 129 and 155 GeV. Being mostly singlet-like its couplings to SM particles are suppressed enough not to represent any danger with respect to the LHC Higgs exclusion limits in this mass range. The benchmark points are ordered in terms of increasing stop mixing X_t scaled by the geometric mean $m_{\tilde{t}}$ of the soft SUSY breaking stop mass parameters. The gluino mass is about 700 GeV for all the points and recall that the squark and slepton masses not shown are all about 1 TeV.

NMP1 with $(\lambda, \kappa) = (0.64, 0.25)$ and $\tan\beta = 3$ is an example of a benchmark point where a SM-like Higgs boson with mass 124.5 GeV can be achieved in the pure NMSSM with relatively small mixing, $X_t/m_{\tilde{t}} = 1.74$. Due to a slightly larger coupling of the SM-like Higgs boson to down-type quarks in this scenario, the decay into $b\bar{b}$ is enhanced compared to the SM and also the corresponding branching ratio (normalised to the SM) of $R_{b\bar{b}} = 1.08$. As the decay into $b\bar{b}$ contributes dominantly to the total width, its enhanced value leads to smaller branching ratios into ZZ, WW, $R_{VV} = 0.94$ $(V = W, Z)$. The partial width into photons, however, is enhanced compared to the SM due to the additional SUSY particle loops contributing to the Higgs–$\gamma\gamma$ coupling with the main enhancement induced by the chargino loops, so that in the end the branching ratio into photons is slightly larger than in the SM, $R_{\gamma\gamma} = 1.03$. As for the gluon fusion cross-section, which is dominated by the (s)top quark loops at small $\tan\beta$, it is almost the same as in the SM, with $R_{\sigma_{gg}} = 0.97$. This is because the H_1 couples with SM-strength to the top quarks and the effect of the additional squark loops is small. Due to the smaller branching ratios into VV, in particular the dominating one into WW, the total Higgs production cross-section is estimated to be smaller than in the SM, $R_{\sigma_{tot}} = 0.92$, which is compatible with LHC constraints. The heavier stop mass here of 782 GeV is a little uncomfortable from the point of view of fine-tuning, but not too bad.

NMP2 with $(\lambda, \kappa) = (0.60, 0.18)$ and $\tan\beta = 2$ shows a 126.5 GeV Higgs which has almost SM-like branching ratios into massive vector bosons, $R_{VV} = 1.02$. While it will be difficult to distinguish this Higgs boson from the SM through the decays into WW, ZZ, the branching

Table 6
NMSSM benchmark points with the lightest Higgs boson being SM-like near 125 GeV.

Point	NMP1	NMP2	NMP3
$\tan\beta$	3	2	2
$\mu_{\rm eff}$ [GeV]	200	200	200
λ	0.64	0.6	0.57
κ	0.25	0.18	0.2
A_λ [GeV]	560	405	395
A_κ [GeV]	−10	−10	−80
$M_{\tilde{Q}_3}$ [GeV]	650	700	530
$M_{\tilde{t}_R}$ [GeV]	650	700	530
M_1 [GeV]	106	91	115
M_2 [GeV]	200	200	200
M_3 [GeV]	600	600	600
SM-like Higgs boson			
M_{H_1} [GeV]	124.5	126.5	124.6
$R_{\gamma\gamma}(H_1)$	1.03	1.20	1.42
$R_{VV}(H_1)$	0.94	1.02	1.12
$R_{b\bar{b}}(H_1)$	1.08	1.05	1.01
$R_{\Gamma_{tot}}(H_1)$	1.05	0.96	0.78
$R_{\sigma_{gg}}(H_1)$	0.97	0.96	0.77
$R_{incl}R_{\gamma\gamma}(H_1)$	1.00	1.15	1.11
$R_{incl}R_{VV}(H_1)$	0.91	0.98	0.88
$R_{\sigma_{tot}}(H_1)$	0.92	0.99	0.89
Remaining Higgs spectrum			
M_{H_2} [GeV]	155	132	129
M_{H_3} [GeV]	637	465	456
M_{A_1} [GeV]	128	116	168
M_{A_2} [GeV]	634	463	454
$M_{H^\pm}$ [GeV]	626	454	447
Sparticle masses and stop mixing			
$m_{\tilde{g}}$ [GeV]	700	701	696
$m_{\tilde{\chi}_1^\pm}$ [GeV]	137	131	131
$m_{\tilde{\chi}_2^\pm}$ [GeV]	281	284	284
$m_{\tilde{\chi}_1^0}$ [GeV]	78	68	85
$m_{\tilde{\chi}_2^0}$ [GeV]	134	127	140
$m_{\tilde{\chi}_3^0}$ [GeV]	201	169	178
$m_{\tilde{\chi}_4^0}$ [GeV]	−231	−232	−227
$m_{\tilde{\chi}_5^0}$ [GeV]	292	290	290
$m_{\tilde{b}_1}$ [GeV]	667	715	538
$m_{\tilde{b}_2}$ [GeV]	1014	1015	1011
$m_{\tilde{t}_1}$ [GeV]	548	587	358
$m_{\tilde{t}_2}$ [GeV]	782	838	686
$X_t/m_{\tilde{t}}$	1.74	1.86	2.26
Relic density			
Ωh^2	0.9819	0.1170	0.1100

ratio into $\gamma\gamma$ is significantly larger than the SM value, $R_{\gamma\gamma} = 1.20$, leading to an enhanced number of events in the photon final state, $R_{\sigma_{incl}} R_{\gamma\gamma} = 1.15$. The reason for the increased $\gamma\gamma$ branching ratio is an enhanced photonic decay width due to positive contributions from the SUSY loops not present in the SM, in particular from the chargino loops, and a reduced total width of $R_{\Gamma_{tot}} = 0.96$. The slight deviation of the branching ratio into $b\bar{b}$ from the SM value, $R_{b\bar{b}} = 1.05$, is within our theoretical error estimate. The gluon fusion production cross-section ratio ends up being close to the SM value for the same reasons as for NMP1, $R_{\sigma_{gg}} = 0.96$. Due to the SM-like decays into massive vector bosons the total Higgs cross-section times branching ratios, which is mainly influenced by the branching ratio into WW, is estimated to be very close to the SM value, $R_{\sigma_{tot}} = 0.99$. The heavier stop mass here of 838 GeV is becoming more uncomfortable from the point of view of fine-tuning.

NMP3 with $(\lambda, \kappa) = (0.57, 0.20)$ and $\tan\beta = 2$ shows a 124.6 GeV Higgs boson. Its distinguishing features are a large stop mixing $X_t/m_{\tilde{t}} = 2.26$ and a considerably enhanced branching ratio (normalised to the SM) into photons, $R_{\gamma\gamma} = 1.42$. The large mixing helps to increase the Higgs boson mass as in Eq. (2.8) and consequently allows the stop masses to be reduced, with the heavier stop mass of 686 GeV being apparently more acceptable from the point of view of fine-tuning, but at the price of an increased stop mixing angle. The coupling of the SM-like Higgs boson to down-type fermions is reduced by about 15% compared to the SM so that the total Higgs width dominated by the decay into $b\bar{b}$ is reduced, $R_{\Gamma_{tot}} = 0.78$ (normalised to the SM). Also the couplings to massive gauge bosons are reduced by 6% implying smaller decay rates into WW, ZZ. The branching ratios (normalised to the SM) into WW, ZZ are, however, enhanced, $R_{VV} = 1.12$. This is due to the reduced total width. The large enhancement of $R_{\gamma\gamma}$ is a combination of positive contributions from the SUSY particle loops, mainly charginos, together with a reduced total width.[5] While the coupling to the top quarks is almost SM-like negative contributions from the stop quark loops with relatively light stops and a large Higgs coupling to these states in this scenario decrease the gluon fusion cross-section[6] so that it amounts only to about 77% of the SM value, leading to only ∼10% more events in the $\gamma\gamma$ final state compared to the SM, $R_{\sigma_{incl}} R_{\gamma\gamma} = 1.11$, whereas the number of WW events is suppressed, $R_{\sigma_{incl}} R_{VV} = 0.88$. Thanks to the enhanced branching ratios into $\gamma\gamma$, ZZ and WW, a total cross-section times branching ratios still compatible with the LHC searches is achieved, $R_{\sigma_{tot}} = 0.89$.

5.2. *NMSSM with second lightest Higgs being SM-like*

Table 7 shows three points NMP4, NMP5, NMP6 which satisfy NMSSM perturbativity up to the GUT scale and lead to the SM-like Higgs boson always being the second lightest one H_2 near 125 GeV. The mass of the lightest Higgs boson H_1 is of about 90–96 GeV. We have verified in each case that H_1 is not in conflict with LEP limits due to its singlet character and hence strongly reduced couplings to the SM particles. The gluino mass for these points ranges

[5] The phenomenon of an enhanced decay width into photons due to a suppressed decay into $b\bar{b}$ has also been discussed in [101] for the lighter Higgs H_1 and in [6] for H_2 as well as in [4].

[6] Note that (s)bottom loops only play a minor role in all our scenarios as we have small values of $\tan\beta$.

Table 7
NMSSM benchmark points with the second lightest Higgs boson being SM-like near 125 GeV.

Point	NMP4	NMP5	NMP6
$\tan\beta$	3	3	2
$\mu_{\rm eff}$ [GeV]	200	200	140
λ	0.67	0.66	0.55
κ	0.1	0.12	0.31
A_λ [GeV]	650	650	210
A_κ [GeV]	−10	−10	−210
$M_{\tilde{Q}_3}$ [GeV]	600	600	800
$M_{\tilde{t}_R}$ [GeV]	600	600	600
M_1 [GeV]	200	200	145
M_2 [GeV]	400	400	300
M_3 [GeV]	600	600	800
SM-like Higgs boson			
M_{H_2} [GeV]	123.8	126.5	124.5
$R_{\gamma\gamma}(H_2)$	1.06	1.15	1.39
$R_{VV}(H_2)$	1.01	1.06	1.10
$R_{b\bar{b}}(H_2)$	1.05	1.03	1.00
$R_{\Gamma_{tot}}(H_2)$	0.99	0.93	0.81
$R_{\sigma_{gg}}(H_2)$	1.00	0.96	0.91
$R_{incl}R_{\gamma\gamma}(H_2)$	1.06	1.11	1.26
$R_{incl}R_{VV}(H_2)$	1.01	1.03	1.00
$R_{\sigma_{tot}}(H_2)$	1.01	1.03	1.02
Remaining Higgs spectrum			
M_{H_1} [GeV]	90	96	90
M_{H_3} [GeV]	654	656	325
M_{A_1} [GeV]	86	93	249
M_{A_2} [GeV]	655	656	317
$M_{H^\pm}$ [GeV]	643	645	312
Sparticle masses and stop mixing			
$m_{\tilde{g}}$ [GeV]	699	699	875
$m_{\tilde{\chi}_1^\pm}$ [GeV]	182	182	114
$m_{\tilde{\chi}_2^\pm}$ [GeV]	438	438	342
$m_{\tilde{\chi}_1^0}$ [GeV]	69	78	80
$m_{\tilde{\chi}_2^0}$ [GeV]	173	175	163
$m_{\tilde{\chi}_3^0}$ [GeV]	233	238	−169
$m_{\tilde{\chi}_4^0}$ [GeV]	−241	−239	197
$m_{\tilde{\chi}_5^0}$ [GeV]	438	438	343
$m_{\tilde{b}_1}$ [GeV]	619	617	822
$m_{\tilde{b}_2}$ [GeV]	1013	1013	827
$m_{\tilde{t}_1}$ [GeV]	517	483	549
$m_{\tilde{t}_2}$ [GeV]	724	741	892
$X_t/m_{\tilde{t}}$	1.56	1.89	−1.83
Relic density			
Ωh^2	0.0999	0.1352	0.1258

from 700 to 875 GeV[7] and, as in all cases, the squark and slepton masses not shown are all about 1 TeV.

NMP4 with $(\lambda, \kappa) = (0.67, 0.10)$ and $\tan\beta = 3$ shows a 123.8 GeV Higgs boson with almost SM-like branching ratios into massive vector bosons, $R_{VV} = 1.01$. It differs from the SM Higgs by its slightly larger value of branching ratio (normalised to the SM) into photons, $R_{\gamma\gamma} = 1.06$, which is due to the positive SUSY particle loop contributions, mainly from chargino loops. The combined effect of the sbottom and stop loops in addition to the heavy quark loops is such that the gluon fusion production cross-section is SM-like. The total production cross-section times branching ratios is near the SM value, $R_{\sigma_{tot}} = 1.01$. With $X_t/m_{\tilde{t}} = 1.56$, the heavier stop mass here of 724 GeV is a little uncomfortable from the point of view of fine-tuning, but not too bad. While this Higgs boson will be difficult to be distinguished from the SM Higgs state, the main new interesting feature is the appearance of two light bosons with $M_{H_1} = 90$ GeV and $M_{A_1} = 86$ GeV which are predominantly composed of singlet S and therefore would have escaped detection at LEP.

NMP5 with $(\lambda, \kappa) = (0.66, 0.12)$ and $\tan\beta = 3$ shows a 126.5 GeV Higgs boson which is also hard to distinguish from the SM Higgs due to its gauge boson branching ratios being close to the SM values, $R_{VV} = 1.06$. However the one into $\gamma\gamma$ is significantly larger, $R_{\gamma\gamma} = 1.15$, which is the combined effect of an enhancement due to SUSY particle loops and a smaller total decay width, $R_{\Gamma_{tot}} = 0.93$, mainly due to a smaller decay width into $b\bar{b}$ as consequence of a reduced Higgs coupling to down-type fermions. With the additional suppression of other decay channels, in the end the branching ratio into $b\bar{b}$ is slightly larger than in the SM, $R_{b\bar{b}} = 1.03$. The gluon fusion production cross-section is only slightly smaller than in the SM, $R_{\sigma_{gg}} = 0.96$. Together with the enhanced branching ratios into gauge bosons, we estimate the total production Higgs cross-section times branching ratios to be close to the SM value, $R_{\sigma_{tot}} = 1.03$, while the number of events in the $\gamma\gamma$ final state is enhanced compared to the SM, $R_{\sigma_{incl}} R_{\gamma\gamma} = 1.11$. The heavier stop mass here of 741 GeV is a little uncomfortable from the point of view of fine-tuning, but not too bad. There are two light bosons with $M_{H_1} = 96$ GeV and $M_{A_1} = 93$ GeV which are predominantly composed of singlet S and therefore would have escaped detection at LEP.

NMP6 with $(\lambda, \kappa) = (0.55, 0.31)$ and a lower $\tan\beta = 2$ shows a 124.5 GeV Higgs boson which can be distinguished from the SM Higgs state by its branching ratios (normalised to the SM) into massive gauge bosons of $R_{VV} = 1.10$ and in particular by into photons. With $R_{\gamma\gamma} = 1.39$ the $\gamma\gamma$ branching ratio shows a very significant enhancement. Once again this is the combined effect of a reduction of the total width, $R_{\Gamma_{tot}} = 0.81$, and a larger Higgs to photon coupling due to SUSY particle loops. The former results from a reduced Higgs coupling to down-type quarks, suppressing the partial width into $b\bar{b}$. Nevertheless, the branching ratio for this final state is SM-like, $R_{b\bar{b}} = 1.00$, due to the additional suppression of other decay channels contributing to Γ_{tot}. In this scenario, the squark loops reduce the gluon fusion cross-section by about 9%, $R_{\sigma_{gg}} = 0.91$, resulting in an estimate of the total cross-section times branching ratios which due to the enhanced branching ratios into vector bosons is very close to the SM, $R_{\sigma_{tot}} = 1.02$. The number of photon final state events, however, is enhanced by considerable 26% compared to

[7] The higher value of the gluino mass for the benchmark point NMP6 results from the gaugino mass chosen to be $M_3 = 800$ GeV in order to fulfill approximate GUT relations between the soft SUSY breaking gaugino masses. This condition is not necessary, however, and choosing a lower value of M_3 and hence $m_{\tilde{g}}$ does not change our results in the Higgs sector.

the SM. The mixing of $X_t/m_{\tilde{t}} = -1.83$ leads to stop masses of 549 and 892 GeV, the latter making the scenario more uncomfortable from the point of view of fine-tuning. Interestingly, in this case there is only one light boson with $M_{H_1} = 90$ GeV, which is predominantly singlet-like and therefore would have escaped detection at LEP.

5.3. NMSSM-with-extra-matter and second Higgs being SM-like

Table 8 shows three points NMP7, NMP8, NMP9 which satisfy perturbativity up to the GUT scale providing that the NMSSM is supplemented by three $SO(10)$ 10-plets as in Table 3. The only slightly larger value of $\lambda = 0.68$–0.69 allows the extra matter to be at or above the TeV scale. It therefore may play no role in any LHC phenomenology, apart from the indirect effect of allowing λ to be a bit larger than allowed by the usual requirement of perturbativity in the NMSSM with no extra matter. All these points lead to the SM-like Higgs boson always being the second lightest one H_2 near 125 GeV. The points are ordered in terms of increasing stop mixing X_t scaled by $m_{\tilde{t}}$. In two of the benchmark scenarios H_1 is light with masses of 83 and 93 GeV, respectively, in one scenario it is almost degenerate with H_2 with a mass of 124 GeV. In all these cases we have verified that such light bosons are sufficiently singlet-like that they would have been produced with sufficiently low rates in order not to be in conflict with LEP and LHC searches. The gluino mass ranges between about 700 and 880 GeV. Recall that the squark and slepton masses not shown are all about 1 TeV.

NMP7 with $(\lambda, \kappa) = (0.68, 0.06)$ and $\tan\beta = 2$ involves a 124.5 GeV Higgs boson which will be difficult to be distinguished from the SM Higgs by branching ratios into massive vector bosons (normalised to the SM) of $R_{VV} = 1.06$. The reduced coupling to down-type quarks leads to a smaller decay width into $b\bar{b}$ and hence a smaller total width than in the SM, $R_{\Gamma_{tot}} = 0.90$. The combined effect of a reduced decay into $b\bar{b}$ and a positive contribution of, in particular, chargino loops to the Higgs coupling to photons leads to a significantly enhanced branching ratio into photons compared to the SM with $R_{\gamma\gamma} = 1.17$, which can be used to distinguish this NMSSM scenario from the SM case through the enhanced number of events in the photon final state, $R_{\sigma_{incl}} R_{\gamma\gamma} = 1.20$. The H_2 coupling to up-type quarks is SM-like so that the gluon fusion production dominated by (s)top quark loops is not altered. With a small positive contribution from stop loops this leads to a 3% enhancement, $R_{\sigma_{gg}} = 1.03$, and implies an estimated total Higgs production cross-section times branching ratio (normalised to the SM value) of $R_{\sigma_{tot}} = 1.10$. The stop masses are almost 800 GeV making this point appear to be somewhat fine-tuned. However, the absence of any stop mixing $X_t/m_{\tilde{t}} = 0$, which is the main feature of this point, serves to ameliorate the fine-tuning. Note that, in the MSSM, a 125 GeV Higgs with zero stop mixing would be impossible. In addition there are two light bosons with $M_{H_1} = 93$ GeV and $M_{A_1} = 99$ GeV which are predominantly singlet-like and therefore would have escaped detection at LEP.

NMP8 with $(\lambda, \kappa) = (0.69, 0.125)$ and $\tan\beta = 2$ involves a 126.2 GeV Higgs boson. The main features of this scenario are reduced branching ratios not only into massive gauge bosons, $R_{VV} = 0.87$, but also into photons, $R_{\gamma\gamma} = 0.87$, and particularly light stop masses with the lighter $m_{\tilde{t}_1} = 104$ GeV. The branching ratio reductions are due to an enhanced decay width into $b\bar{b}$ because of a slightly larger coupling to down-type quarks than in the SM. In addition, the decay into photons is reduced because of smaller H_2 couplings to up-type quarks and negative stop quark loop contributions in this scenario. In the gluon fusion production the positive contributions from the stop quark loops counterbalance the reduction of the cross-section because

Table 8
NMSSM-with-extra-matter benchmark points with second lightest Higgs being SM-like near 125 GeV.

Point	NMP7	NMP8	NMP9
$\tan\beta$	2	2	3
$\mu_{\rm eff}$ [GeV]	200	190	200
λ	0.68	0.69	0.68
κ	0.06	0.125	0.2
A_λ [GeV]	500	420	600
A_κ [GeV]	−100	−100	−10
$M_{\tilde{Q}_3}$ [GeV]	750	400	500
$M_{\tilde{t}_R}$ [GeV]	750	230	500
M_1 (GeV)	200	120	135
M_2 (GeV)	400	335	200
M_3 (GeV)	800	800	600
SM-like Higgs boson			
M_{H_2} [GeV]	124.5	126.2	125.8
$R_{\gamma\gamma}(H_2)$	1.17	0.87	1.78
$R_{VV}(H_2)$	1.06	0.87	1.41
$R_{b\bar{b}}(H_2)$	1.02	1.12	0.84
$R_{\Gamma_{tot}}(H_2)$	0.90	1.06	0.53
$R_{\sigma_{gg}}(H_2)$	1.03	1.01	0.79
$R_{incl}R_{\gamma\gamma}(H_2)$	1.20	0.86	1.39
$R_{incl}R_{VV}(H_2)$	1.09	0.87	1.11
$R_{\sigma_{tot}}(H_2)$	1.10	0.87	1.13
Remaining Higgs spectrum			
M_{H_1} [GeV]	93	83	124
M_{H_3} [GeV]	495	434	641
M_{A_1} [GeV]	99	139	119
M_{A_2} [GeV]	503	438	640
$M_{H^\pm}$ [GeV]	485	422	629
Sparticle masses and stop mixing			
$m_{\tilde{g}}$ [GeV]	882	877	695
$m_{\tilde{\chi}_1^\pm}$ [GeV]	179	159	137
$m_{\tilde{\chi}_2^\pm}$ [GeV]	439	379	281
$m_{\tilde{\chi}_1^0}$ [GeV]	66	76	81
$m_{\tilde{\chi}_2^0}$ [GeV]	160	120	143
$m_{\tilde{\chi}_3^0}$ [GeV]	231	191	185
$m_{\tilde{\chi}_4^0}$ [GeV]	−248	−233	−237
$m_{\tilde{\chi}_5^0}$ [GeV]	440	380	291
$m_{\tilde{b}_1}$ [GeV]	779	379	514
$m_{\tilde{b}_2}$ [GeV]	1022	999	1011
$m_{\tilde{t}_1}$ [GeV]	786	104	391
$m_{\tilde{t}_2}$ [GeV]	797	442	634
$X_t/m_{\tilde{t}}$	0	1.48	1.77
Relic density			
Ωh^2	0.0973	0.1101	0.1031

of the smaller H_2 coupling to top quarks, so that the ratio to the SM cross-section is nearly one, $R_{\sigma_{gg}} = 1.01$. However the smaller branching ratios into WW, ZZ and $\gamma\gamma$ drive the total cross-section times branching ratios down to $R_{\sigma_{tot}} = 0.87$ (normalised to the SM). This is still compatible with the present LHC searches though, according to our criteria. With $X_t/m_{\tilde{t}} = 1.48$, the interesting feature of this scenario is the very light stop which is close enough in mass to the lightest neutralino in order to dominantly decay via the flavour changing neutral current decay into charm and $\tilde{\chi}_1^0$. Such a light stop is not excluded in this decay channel by the present LHC searches. The correct amount of dark matter relic density is here achieved through $\tilde{t}_1\tilde{\chi}_1^0$ co-annihilation into W^+b. Also in this scenario we have two light bosons with $M_{H_1} = 83$ GeV and $M_{A_1} = 139$ GeV which are predominantly singlet-like and hence not in conflict with LEP and LHC exclusion limits.

NMP9 with $(\lambda, \kappa) = (0.68, 0.20)$ and $\tan\beta = 3$ involves a 125.8 GeV Higgs boson. The main features of this scenario are the near degeneracy of the physical SM-like Higgs with a lighter Higgs boson of mass $M_{H_1} = 124$ GeV as well as considerably enhanced branching ratios (normalised to the SM) into photons, $R_{\gamma\gamma} = 1.78$, and into massive gauge bosons, $R_{VV} = 1.41$. Due to the near degeneracy of H_1 and H_2, and the associated large mixing, each state contains a significant singlet component, with the most SM-like Higgs H_2 coupling only with about 60% of the SM strength to down-type quarks so that both the decay width into $b\bar{b}$ and the total width are reduced, $R_{b\bar{b}} = 0.84$ and $R_{\Gamma_{tot}} = 0.53$, and hence the branching ratios into gauge bosons enhanced. As the H_2 coupling to top quarks is also reduced the gluon fusion production cross-section goes down supplemented by a small negative contribution from stop loops, so that in the end we have $R_{\sigma_{gg}} = 0.79$. Nevertheless, due to the enhanced branching ratios, the combined cross-section times branching ratios is compatible with LHC searches as $R_{\sigma_{tot}} = 1.13$. Particularly interesting is the still considerably enhanced number of photon final state events compared to the SM, $R_{\sigma_{incl}} R_{\gamma\gamma} = 1.39$, which is a distinctive feature of this scenario. Also the H_1 state is consistent with LHC searches as its couplings to up-type quarks are reduced so that it cannot be produced with sufficiently large rate to yield a second signal at the LHC. In addition there is a singlet-dominated boson of mass $M_{A_1} = 119$ GeV. With $X_t/M_{m_{\tilde{t}}} = 1.77$, and the heavier stop mass here of 634 GeV, and a gluino mass of 695 GeV, there is relatively little fine-tuning for this point.

5.4. NMSSM-with-extra-matter and lightest Higgs being SM-like

Table 9 shows three points NMP10, NMP11, NMP12 which satisfy perturbativity up to the GUT scale providing that the NMSSM is supplemented by three $SO(10)$ 10-plets as in Table 2. The larger value of $\lambda = 0.7$, held fixed for all these points, requires the extra matter to be close to the electroweak scale. It may therefore be expected to play a role in LHC phenomenology. All these points lead to the SM-like Higgs always being the lightest one, H_1, near 125 GeV. The points are ordered in terms of increasing stop mixing X_t scaled by $m_{\tilde{t}}$. The second lightest Higgs boson has masses in the range of about 130 to 145 GeV and, due to its singlet nature, we have checked that it is in accordance with present LHC exclusion limits. The gluino mass for these benchmark points is about 700 GeV and recall that the squark and slepton masses not shown are all about 1 TeV.

NMP10 with $(\lambda, \kappa) = (0.70, 0.20)$ and $\tan\beta = 2$ involves a 123.6 GeV Higgs which is SM-like in its decays into massive vector bosons and b quarks with the normalised branching ratios given by $R_{VV} = 1.01$ and $R_{b\bar{b}} = 1.04$. The branching ratio into photons, however, is enhanced

Table 9
NMSSM-with-extra-matter benchmark points with the lightest Higgs being SM-like near 125 GeV.

Point	NMP10	NMP11	NMP12
$\tan\beta$	2	2	3
$\mu_{\rm eff}$ [GeV]	200	200	200
λ	0.7	0.7	0.7
κ	0.2	0.2	0.25
A_λ [GeV]	405	405	560
A_κ [GeV]	−10	−10	−10
$M_{\tilde{Q}_3}$ [GeV]	600	510	500
$M_{\tilde{t}_R}$ [GeV]	600	510	500
M_1 [GeV]	120	120	125
M_2 [GeV]	200	200	200
M_3 [GeV]	600	600	600
SM-like Higgs boson			
M_{H_1} [GeV]	123.6	123.5	123.7
$R_{\gamma\gamma}(H_1)$	1.15	2.00	1.24
$R_{VV}(H_1)$	1.01	1.48	1.09
$R_{b\bar{b}}(H_1)$	1.04	0.82	1.01
$R_{\Gamma_{tot}}(H_1)$	0.98	0.40	0.90
$R_{\sigma_{gg}}(H_1)$	1.07	0.71	1.00
$R_{incl}R_{\gamma\gamma}(H_1)$	1.21	1.39	1.23
$R_{incl}R_{VV}(H_1)$	1.07	1.03	1.09
$R_{\sigma_{tot}}(H_1)$	1.08	1.06	1.10
Remaining Higgs spectrum			
M_{H_2} [GeV]	133	136	144
M_{H_3} [GeV]	468	458	629
M_{A_1} [GeV]	129	129	133
M_{A_2} [GeV]	469	459	626
$M_{H^\pm}$ [GeV]	456	445	615
Sparticle masses and stop mixing			
$m_{\tilde{g}}$ [GeV]	686	696	696
$m_{\tilde{\chi}_1^\pm}$ [GeV]	131	131	137
$m_{\tilde{\chi}_2^\pm}$ [GeV]	284	283	281
$m_{\tilde{\chi}_1^0}$ [GeV]	82	82	83
$m_{\tilde{\chi}_2^0}$ [GeV]	137	137	141
$m_{\tilde{\chi}_3^0}$ [GeV]	175	175	198
$m_{\tilde{\chi}_4^0}$ [GeV]	−241	−240	−236
$m_{\tilde{\chi}_5^0}$ [GeV]	291	291	293
$m_{\tilde{b}_1}$ [GeV]	622	525	516
$m_{\tilde{b}_2}$ [GeV]	1013	1011	1011
$m_{\tilde{t}_1}$ [GeV]	630	445	413
$m_{\tilde{t}_2}$ [GeV]	645	620	624
$X_t/m_{\tilde{t}}$	0	1.33	1.57
Relic density			
Ωh^2	0.1135	0.1161	0.1050

with (normalised to the SM) $R_{\gamma\gamma} = 1.15$. This is a consequence of positive contributions from chargino loops to the $H_1\gamma\gamma$ coupling. The cross-section ratio $R_{\sigma_{gg}} = 1.07$ is somewhat larger than in the SM because of positive contributions from the stop loops. Together with the SM-like branching ratios into massive gauge bosons and an enhanced one into $\gamma\gamma$, in the end the estimated total Higgs cross-section times branching ratios is not far from the SM value, $R_{\sigma_{tot}} = 1.08$. The number of photon events, however, is enhanced by significant 21% compared to the SM. The stop masses are 630 and 645 GeV with the gluino mass 686 GeV, which does not require fine-tuning, since there is no stop mixing $X_t/m_{\tilde{t}} = 0$. This of course would be impossible in the MSSM. The reason it is possible here is the large $\lambda = 0.7$, and low $\tan\beta = 2$, which together provide a nice tree-level Higgs mass contribution as in Eq. (1.2). The heavier Higgs H_2 is not too far away at 133 GeV but, of course, is singlet dominated and hence hard to discover.

NMP11 with $(\lambda, \kappa) = (0.70, 0.20)$ and $\tan\beta = 2$ involves a 123.5 GeV Higgs. Here we have a scenario with a strong singlet–doublet mixing, this time for the lightest Higgs boson H_1. As a consequence, its couplings to down-type quarks are reduced implying a smaller decay width into $b\bar{b}$ leading to a total width of only about 40% of the SM value, $R_{\Gamma_{tot}} = 0.40$. The branching ratios into massive gauge bosons are therefore significantly enhanced, $R_{VV} = 1.48$, despite H_1 also having reduced couplings to gauge bosons. The most interesting feature, however, is the enhancement of the branching ratio into photons by a factor 2, $R_{\gamma\gamma} = 2.00$, due to the combined effect of the smaller total width and the positive chargino loop contributions which counterbalance the loss in the H_1 coupling to $\gamma\gamma$ because of a reduced coupling to top quarks. The cross-section ratio $R_{\sigma_{gg}} = 0.71$ results from the reduced top loop contributions which cannot be made up for by positive contributions from the squark loops. While the number of WW final states and the total cross-section times branching ratios, dominated by the decay into WW, end up near their corresponding SM values, the number of photonic events is enhanced by as much as 39%, providing a distinctive feature for this benchmark point. The nearby H_2 state with 136 GeV represents no danger with respect to LHC exclusion limits as its couplings to SM particles are reduced implying small enough production rates to be safe. With $X_t/m_{\tilde{t}} = 1.33$, and a heavier stop mass of 620 GeV, and a gluino mass of 696 GeV, this is a natural point without much fine-tuning.

NMP12 with $(\lambda, \kappa) = (0.70, 0.25)$ and $\tan\beta = 3$ involves a 123.7 GeV Higgs boson which is harder to distinguish from the SM Higgs by branching ratios into massive vector bosons (normalised to the SM) of $R_{VV} = 1.09$. However with $R_{\gamma\gamma} = 1.24$ the branching ratio into photons is significantly different from the SM and enhanced once again because of positive chargino loop contributions. As the H_1 coupling to top quarks is the same as in the SM and the marginal contributions from squark loops add up to almost zero, the gluon production cross-section is the same as in the SM, $R_{\sigma_{gg}} = 1.00$. With the enhanced branching ratios into vector bosons the total production times branching ratios ends up to be larger than in the SM, $R_{\sigma_{tot}} = 1.10$, and the number of photon final state events is enhanced by significant 23%. The normalized mixing $X_t/m_{\tilde{t}} = 1.57$ features stop masses of 413 and 624 GeV. With the gluino mass of 696 GeV these are quite natural values which does not require fine-tuning.

6. Summary and conclusion

The recent ATLAS and CMS indications of a SM-like Higgs boson near 125 GeV are consistent not only with the SM Higgs but also a SUSY Higgs. If it is a SUSY Higgs, the question is what sort of SUSY theory is responsible for it, and what part of parameter space of the SUSY

theory does it correspond to? In this paper we have been guided by both naturalness and minimality to consider the possibility that the SM-like Higgs arises from the NMSSM. Minimality alone would suggest the MSSM, however a 125 GeV Higgs can only be achieved in the MSSM with stops necessarily having some mixing and mass parameters above 1 TeV, which leads to some considerable amount of tuning. By contrast, the NMSSM, which includes only one additional singlet superfield S, allows a 125 GeV Higgs to arise with all stop masses and mixing below 1 TeV. Thus the NMSSM appears to be the best compromise between naturalness and minimality that can account for a 125 GeV SM-like Higgs boson, with the SM itself excluded on naturalness grounds.

Given that the NMSSM is a well-motivated SUSY theory, the next question is what part of NMSSM parameter space does the SM-like Higgs boson near 125 GeV correspond to? Clearly on naturalness grounds we are led to consider large values of λ and low values of $\tan\beta$, in order to maximise the tree-level contribution to the Higgs mass in Eq. (1.2). However λ cannot be too large otherwise it would blow up below the GUT scale which we regard as unacceptable. Therefore it is important to know just how large λ can be, as a function of κ and $\tan\beta$. We have studied this question using two-loop RGEs and found that it cannot be as large as is often assumed in the literature. However, if the SUSY desert contains extra matter, then λ can be increased, depending on the precise mass threshold of the extra matter, which is a new result of this paper.

Assuming the NMSSM with large values of λ and low values of $\tan\beta$, which may or may not require extra matter, another key requirement for us is having stop masses and mixings below 1 TeV, on naturalness grounds. Since the LHC has already placed strong limits on the first and second family squarks we are therefore led to consider a general NMSSM, i.e. not the constrained NMSSM. Given the rich parameter space of the NMSSM, it is practically impossible to perform scans over all NMSSM parameter space to identify which regions are consistent with a 125 GeV Higgs. Instead we have adopted a different strategy in this paper, namely that of using benchmark points. Each benchmark point in the NMSSM parameter space allows everything to be calculated to the standard of precision that is currently available. For each benchmark point, the nature and properties of the SM-like NMSSM Higgs boson can be scrutinised and compared to the SM expectation, which could allow the NMSSM Higgs to be resolved from the SM Higgs boson by future LHC searches and measurements. It is possible for experimentalists to use these benchmark points to test the NMSSM in different regions of the parameter space by performing studies beyond what, as mere theorists, we are capable of.

Motivated by these considerations we have proposed four sets of benchmark points corresponding to the SM-like Higgs being the lightest or the second lightest in the NMSSM or the NMSSM-with-extra-matter. Points NMP1, NMP2, NMP3 are for the NMSSM with the lightest Higgs being SM-like near 125 GeV. Points NMP4, NMP5, NMP6 are for the NMSSM with the second lightest Higgs being SM-like near 125 GeV. Points NMP7, NMP8, NMP9 are for the NMSSM-with-extra-matter at or above the TeV scale where the second lightest Higgs is SM-like near 125 GeV. Points NMP10, NMP11, NMP12 are for the NMSSM-with-extra-matter close to the electroweak scale and the lightest Higgs being SM-like near 125 GeV. For each of these points we have discussed how the NMSSM Higgs boson near 125 GeV may be distinguished from the SM Higgs state in future LHC searches. We have considered both the gluon cross-section and the branching ratios into WW, ZZ and two photons. We also considered a weighted total Higgs cross-section times branching ratios as a measure of how many Higgs events would be observed in current searches.

Each benchmark point, with different values of Higgs cross-sections and branching ratios, acts like a little beacon which in principle can allow experiment to guide us to the correct part of the NMSSM parameter space. It is worth emphasising, however, that the values of R_{VV} and $R_{b\bar{b}}$ quoted here are only accurate to a few percent, as they are obtained by using two different programs for the calculation of the branching ratios, `NMSSMTools` for the NMSSM and `HDECAY` for the SM case, which use different approximations in the calculation of the various partial widths. The differences are always less than or equal to 5% for the quoted values, while the maximum deviations for $R_{\gamma\gamma}$ differ by up to 10%. Although these theoretical uncertainties are well within the expected experimental error for the measurement of these branching ratios at the LHC, it does mean that resolving the NMSSM Higgs from the SM Higgs is going to be challenging. However, in some cases the Higgs branching ratio into two photons may easily be enhanced by a factor of two in the NMSSM, as seen in NMP9 and NMP11. These very large enhancements result in part from the reduction in the bottom quark–antiquark decay rate due to the reduced amount of H_d component in the SM-like Higgs boson. Moreover significant enhancements in the two photon channel are also seen for other points where the $b\bar{b}$ decay rate is not reduced, and this is typically due to the effect of chargino loops.

In general we have taken the stop masses and mixing to be as low as possible, the extreme example of this being NMP8 where the lightest stop is only 104 GeV. We find it remarkable that such light stops are still allowed by current searches, although we would expect stops below 1 TeV, as assumed here, to be discovered soon at the LHC. We look forward to the forthcoming LHC run in 2012 with much excitement.

Acknowledgements

S.F.K. would like to thank S. Belyaev and H. Haber for stimulating discussions. M.M.M. gratefully acknowledges several discussions with G. Bélanger, J. Cao, U. Ellwanger, A. Pukhov and M. Spira. R. Nevzorov would like to thank X. Tata for fruitful discussions. M.M.M. is supported by the DFG SFB/TR9 "Computational Particle Physics". The work of R.N. was supported by the U.S. Department of Energy under Contract DE-FG02-04ER41291. S.F.K. acknowledges partial support from the STFC Consolidated ST/J000396/1 and EU ITN grant UNILHC 237920 (Unification in the LHC era).

Appendix A. Renormalisation group equations to second order

The running of the gauge couplings from the GUT scale to the EW scale is determined by a set of RGEs. In our analysis, we use two-loop RGEs for the gauge and Yukawa couplings. Retaining only λ, κ, h_t, h_b and h_τ the two-loop RGEs in the NMSSM can be written as

$$\begin{aligned}
\frac{dg_i}{dt} &= \frac{\beta_i g_i^3}{(4\pi)^2},\\
\frac{d\lambda}{dt} &= \frac{\lambda}{(4\pi)^2}\left[4\lambda^2 + 2\kappa^2 + 3h_t^2 + 3h_b^2 + h_\tau^2 - 3g_2^2 - \frac{3}{5}g_1^2 + \frac{\beta_\lambda^{(2)}}{(4\pi)^2}\right],\\
\frac{d\kappa}{dt} &= \frac{\kappa}{(4\pi)^2}\left[6\left(\kappa^2+\lambda^2\right) + \frac{1}{(4\pi)^2}\left(18\lambda^2 g_2^2 + \frac{18}{5}\lambda^2 g_1^2\right.\right.\\
&\qquad \left.\left. - \lambda^2\left(12\lambda^2 + 24\kappa^2 + 18h_t^2 + 18h_b^2 + 6h_\tau^2\right) - 24\kappa^4\right)\right],
\end{aligned}$$

$$\frac{dh_t}{dt} = \frac{h_t}{(4\pi)^2}\left[\lambda^2 + 6h_t^2 + h_b^2 - \frac{16}{3}g_3^2 - 3g_2^2 - \frac{13}{15}g_1^2 + \frac{\beta_{h_t}^{(2)}}{(4\pi)^2}\right],$$
$$\frac{dh_b}{dt} = \frac{h_b}{(4\pi)^2}\left[\lambda^2 + h_t^2 + 6h_b^2 + h_\tau^2 - \frac{16}{3}g_3^2 - 3g_2^2 - \frac{7}{15}g_1^2 + \frac{\beta_{h_b}^{(2)}}{(4\pi)^2}\right],$$
$$\frac{dh_\tau}{dt} = \frac{h_\tau}{(4\pi)^2}\left[\lambda^2 + 3h_b^2 + 4h_\tau^2 - 3g_2^2 - \frac{9}{5}g_1^2 + \frac{\beta_{h_\tau}^{(2)}}{(4\pi)^2}\right], \tag{A.1}$$

where $t = \ln[Q/M_X]$; the index i runs from 1 to 3 and is associated with $U(1)_Y$, $SU(2)_W$ and $SU(3)_C$ gauge interactions; $\beta_\lambda^{(2)}$, $\beta_{h_t}^{(2)}$, $\beta_{h_b}^{(2)}$ and $\beta_{h_\tau}^{(2)}$ are the two-loop contributions to the corresponding β-functions.

In the NMSSM the two-loop β-functions of the gauge couplings, $\beta_\lambda^{(2)}$, $\beta_{h_t}^{(2)}$, $\beta_{h_b}^{(2)}$ and $\beta_{h_\tau}^{(2)}$ are given by[8]

$$\beta_3 = -3 + \frac{1}{16\pi^2}\left[14g_3^2 + 9g_2^2 + \frac{11}{5}g_1^2 - 4h_t^2 - 4h_b^2\right],$$
$$\beta_2 = 1 + \frac{1}{16\pi^2}\left[24g_3^2 + 25g_2^2 + \frac{9}{5}g_1^2 - 6h_t^2 - 6h_b^2 - 2h_\tau^2 - 2\lambda^2\right],$$
$$\beta_1 = \frac{33}{5} + \frac{1}{16\pi^2}\left[\frac{88}{5}g_3^2 + \frac{27}{5}g_2^2 + \frac{199}{25}g_1^2 - \frac{26}{5}h_t^2 - \frac{14}{5}h_b^2 - \frac{18}{5}h_\tau^2 - \frac{6}{5}\lambda^2\right], \tag{A.2}$$
$$\begin{aligned}\beta_\lambda^{(2)} = {} & -9h_t^4 - 9h_b^4 - 6h_t^2h_b^2 - 3h_\tau^4 - 8\kappa^4 - \lambda^2\left(9h_t^2 + 9h_b^2 + 3h_\tau^2 + 12\kappa^2 + 10\lambda^2\right) \\ & + 16g_3^2\left(h_t^2 + h_b^2\right) + 6g_2^2\lambda^2 + g_1^2\left(\frac{4}{5}h_t^2 - \frac{2}{5}h_b^2 + \frac{6}{5}h_\tau^2 + \frac{6}{5}\lambda^2\right) \\ & + \frac{15}{2}g_2^4 + \frac{9}{5}g_2^2g_1^2 + \frac{207}{50}g_1^4,\end{aligned}$$
$$\begin{aligned}\beta_{h_t}^{(2)} = {} & -22h_t^4 - 5h_b^4 - 5h_t^2h_b^2 - h_b^2h_\tau^2 - \lambda^2\left(3\lambda^2 + 3h_t^2 + 4h_b^2 + h_\tau^2 + 2\kappa^2\right) \\ & + 16g_3^2h_t^2 + 6g_2^2h_t^2 + g_1^2\left(\frac{6}{5}h_t^2 + \frac{2}{5}h_b^2\right) - \frac{16}{9}g_3^4 + \frac{15}{2}g_2^4 + \frac{2743}{450}g_1^4 \\ & + 8g_3^2g_2^2 + \frac{136}{45}g_3^2g_1^2 + g_2^2g_1^2,\end{aligned}$$
$$\begin{aligned}\beta_{h_b}^{(2)} = {} & -5h_t^4 - 22h_b^4 - 5h_t^2h_b^2 - 3h_b^2h_\tau^2 - 3h_\tau^4 - \lambda^2\left(3\lambda^2 + 4h_t^2 + 3h_b^2 + 2\kappa^2\right) \\ & + 16g_3^2h_b^2 + 6g_2^2h_b^2 + g_1^2\left(\frac{4}{5}h_t^2 + \frac{2}{5}h_b^2 + \frac{6}{5}h_\tau^2\right) - \frac{16}{9}g_3^4 + \frac{15}{2}g_2^4 + \frac{287}{90}g_1^4 \\ & + 8g_3^2g_2^2 + \frac{8}{9}g_3^2g_1^2 + g_2^2g_1^2,\end{aligned}$$
$$\begin{aligned}\beta_{h_\tau}^{(2)} = {} & -9h_b^4 - 3h_t^2h_b^2 - 9h_b^2h_\tau^2 - 10h_\tau^4 - \lambda^2\left(3\lambda^2 + 3h_t^2 + 3h_\tau^2 + 2\kappa^2\right) \\ & + 16g_3^2h_b^2 + 6g_2^2h_\tau^2 + g_1^2\left(-\frac{2}{5}h_b^2 + \frac{6}{5}h_\tau^2\right) + \frac{15}{2}g_2^4 + \frac{27}{2}g_1^4 + \frac{9}{5}g_2^2g_1^2.\end{aligned} \tag{A.3}$$

[8] Note that the two-loop RGE results differ somewhat from the original two-loop RGE results first obtained in the NMSSM by King and White [13], which is why we have written them out explicitly here. Of course the two-loop RGE results including extra matter are new results presented in this paper for the first time.

In the NMSSM with three extra $SO(10)$ 10-plets the two-loop β-functions of the gauge couplings, $\beta_\lambda^{(2)}$, $\beta_{h_t}^{(2)}$, $\beta_{h_b}^{(2)}$ and $\beta_{h_\tau}^{(2)}$ can be written as

$$
\begin{aligned}
\beta_3 &= \frac{1}{16\pi^2}\big[48g_3^2 + 9g_2^2 + 3g_1^2 - 4h_t^2 - 4h_b^2\big],\\
\beta_2 &= 4 + \frac{1}{16\pi^2}\left[24g_3^2 + 46g_2^2 + \frac{18}{5}g_1^2 - 6h_t^2 - 6h_b^2 - 2h_\tau^2 - 2\lambda^2\right],\\
\beta_1 &= \frac{48}{5} + \frac{1}{16\pi^2}\left[24g_3^2 + \frac{54}{5}g_2^2 + \frac{234}{25}g_1^2 - \frac{26}{5}h_t^2 - \frac{14}{5}h_b^2 - \frac{18}{5}h_\tau^2 - \frac{6}{5}\lambda^2\right],\\
\beta_\lambda^{(2)} &= -9h_t^4 - 9h_b^4 - 6h_t^2h_b^2 - 3h_\tau^4 - 8\kappa^4 - \lambda^2\big(9h_t^2 + 9h_b^2 + 3h_\tau^2 + 12\kappa^2 + 10\lambda^2\big)\\
&\quad + 16g_3^2\big(h_t^2 + h_b^2\big) + 6g_2^2\lambda^2 + g_1^2\left(\frac{4}{5}h_t^2 - \frac{2}{5}h_b^2 + \frac{6}{5}h_\tau^2 + \frac{6}{5}\lambda^2\right)\\
&\quad + \frac{33}{2}g_2^4 + \frac{9}{5}g_2^2g_1^2 + \frac{297}{50}g_1^4,\\
\beta_{h_t}^{(2)} &= -22h_t^4 - 5h_b^4 - 5h_t^2h_b^2 - h_b^2h_\tau^2 - \lambda^2\big(3\lambda^2 + 3h_t^2 + 4h_b^2 + h_\tau^2 + 2\kappa^2\big)\\
&\quad + 16g_3^2h_t^2 + 6g_2^2h_t^2 + g_1^2\left(\frac{6}{5}h_t^2 + \frac{2}{5}h_b^2\right) + \frac{128}{9}g_3^4 + \frac{33}{2}g_2^4 + \frac{3913}{450}g_1^4\\
&\quad + 8g_3^2g_2^2 + \frac{136}{45}g_3^2g_1^2 + g_2^2g_1^2,\\
\beta_{h_b}^{(2)} &= -5h_t^4 - 22h_b^4 - 5h_t^2h_b^2 - 3h_b^2h_\tau^2 - 3h_\tau^4 - \lambda^2\big(3\lambda^2 + 4h_t^2 + 3h_b^2 + 2\kappa^2\big)\\
&\quad + 16g_3^2h_b^2 + 6g_2^2h_b^2 + g_1^2\left(\frac{4}{5}h_t^2 + \frac{2}{5}h_b^2 + \frac{6}{5}h_\tau^2\right) + \frac{128}{9}g_3^4 + \frac{33}{2}g_2^4 + \frac{413}{90}g_1^4\\
&\quad + 8g_3^2g_2^2 + \frac{8}{9}g_3^2g_1^2 + g_2^2g_1^2,\\
\beta_{h_\tau}^{(2)} &= -9h_b^4 - 3h_t^2h_b^2 - 9h_b^2h_\tau^2 - 10h_\tau^4 - \lambda^2\big(3\lambda^2 + 3h_t^2 + 3h_\tau^2 + 2\kappa^2\big)\\
&\quad + 16g_3^2h_b^2 + 6g_2^2h_\tau^2 + g_1^2\left(-\frac{2}{5}h_b^2 + \frac{6}{5}h_\tau^2\right) + \frac{33}{2}g_2^4 + \frac{189}{10}g_1^4 + \frac{9}{5}g_2^2g_1^2.
\end{aligned}
\tag{A.4}
\tag{A.5}
$$

References

[1] F. Gianotti, CERN Public Seminar, Update on the Standard Model Higgs Searches in ATLAS, vol. 13, December 2011;
ATLAS Collaboration, ATLAS-CONF-2011-163.

[2] G. Tonelli, CERN Public Seminar, Update on the Standard Model Higgs Searches in CMS, vol. 13, December 2011;
CMS Collaboration, CMS-PAS-HIG-11-032.

[3] G. Kane, P. Kumar, R. Lu, B. Zheng, arXiv:1112.1059 [hep-ph];
I. Gogoladze, Q. Shafi, C.S. Un, arXiv:1112.2206 [hep-ph];
A. Arbey, M. Battaglia, F. Mahmoudi, arXiv:1112.3032 [hep-ph];
A. Arbey, M. Battaglia, A. Djouadi, F. Mahmoudi, J. Quevillon, Phys. Lett. B 708 (2012) 162, arXiv:1112.3028 [hep-ph];
S. Heinemeyer, O. Stal, G. Weiglein, arXiv:1112.3026 [hep-ph];
T. Li, J.A. Maxin, D.V. Nanopoulos, J.W. Walker, arXiv:1112.3024 [hep-ph];
J. Elias-Miro, J.R. Espinosa, G.F. Giudice, G. Isidori, A. Riotto, A. Strumia, Phys. Lett. B 709 (2012) 222, arXiv:1112.3022 [hep-ph];

H. Baer, V. Barger, A. Mustafayev, arXiv:1112.3017 [hep-ph];
C. Englert, T. Plehn, M. Rauch, D. Zerwas, P.M. Zerwas, Phys. Lett. B 707 (2012) 512, arXiv:1112.3007 [hep-ph];
D.E. Kahana, S.H. Kahana, arXiv:1112.2794 [hep-ph];
Z.-z. Xing, H. Zhang, S. Zhou, arXiv:1112.3112 [hep-ph];
T. Moroi, R. Sato, T.T. Yanagida, Phys. Lett. B 709 (2012) 218, arXiv:1112.3142 [hep-ph];
G. Guo, B. Ren, X.-G. He, arXiv:1112.3188 [hep-ph];
C. Cheung, Y. Nomura, arXiv:1112.3043 [hep-ph];
P. Draper, P. Meade, M. Reece, D. Shih, arXiv:1112.3068 [hep-ph];
T. Moroi, K. Nakayama, arXiv:1112.3123 [hep-ph];
P.M. Ferreira, R. Santos, M. Sher, J.P. Silva, arXiv:1112.3277 [hep-ph];
A. Djouadi, O. Lebedev, Y. Mambrini, J. Quevillon, Phys. Lett. B 709 (2012) 65, arXiv:1112.3299 [hep-ph];
M. Carena, S. Gori, N.R. Shah, C.E.M. Wagner, arXiv:1112.3336 [hep-ph];
M. Kadastik, K. Kannike, A. Racioppi, M. Raidal, arXiv:1112.3647 [hep-ph];
S. Akula, B. Altunkaynak, D. Feldman, P. Nath, G. Peim, arXiv:1112.3645 [hep-ph];
O. Buchmueller, R. Cavanaugh, A. De Roeck, M.J. Dolan, J.R. Ellis, H. Flacher, S. Heinemeyer, G. Isidori, et al., arXiv:1112.3564 [hep-ph];
J. Cao, Z. Heng, D. Li, J.M. Yang, arXiv:1112.4391 [hep-ph];
C. Strege, G. Bertone, D.G. Cerdeno, M. Fornasa, R.R. de Austri, R. Trotta, arXiv:1112.4192 [hep-ph];
G. Burdman, C. Haluch, R. Matheus, arXiv:1112.3961 [hep-ph];
A. Arhrib, R. Benbrik, M. Chabab, G. Moultaka, L. Rahili, arXiv:1112.5453 [hep-ph];
A. Bottino, N. Fornengo, S. Scopel, arXiv:1112.5666 [hep-ph].

[4] L.J. Hall, D. Pinner, J.T. Ruderman, arXiv:1112.2703 [hep-ph].

[5] A. Arvanitaki, G. Villadoro, arXiv:1112.4835 [hep-ph].

[6] U. Ellwanger, arXiv:1112.3548 [hep-ph].

[7] J.F. Gunion, Y. Jiang, S. Kraml, arXiv:1201.0982 [hep-ph].

[8] A. Djouadi, Phys. Rept. 459 (2008) 1–241, hep-ph/0503173.

[9] R. Barbieri, G.F. Giudice, Nucl. Phys. B 306 (1988) 63.

[10] B. de Carlos, J.A. Casas, Phys. Lett. B 309 (1993) 320, arXiv:hep-ph/9303291;
P.H. Chankowski, J.R. Ellis, S. Pokorski, Phys. Lett. B 423 (1998) 327, hep-ph/9712234;
R. Barbieri, A. Strumia, Phys. Lett. B 433 (1998) 63, hep-ph/9801353;
G.L. Kane, S.F. King, Phys. Lett. B 451 (1999) 113, hep-ph/9810374;
L. Giusti, A. Romanino, A. Strumia, Nucl. Phys. B 550 (1999) 3, hep-ph/9811386;
Z. Chacko, Y. Nomura, D. Tucker-Smith, Nucl. Phys. B 725 (2005) 207, hep-ph/0504095;
R. Kitano, Y. Nomura, Phys. Lett. B 631 (2005) 58, hep-ph/0509039;
P. Athron, D.J. Miller, Phys. Rev. D 76 (2007) 075010, arXiv:0705.2241 [hep-ph];
S. Cassel, D.M. Ghilencea, G.G. Ross, Nucl. Phys. B 825 (2010) 203, arXiv:0903.1115 [hep-ph];
R. Barbieri, D. Pappadopulo, JHEP 0910 (2009) 061, arXiv:0906.4546 [hep-ph];
M. Asano, H.D. Kim, R. Kitano, Y. Shimizu, JHEP 1012 (2010) 019, arXiv:1010.0692 [hep-ph].

[11] M. Bastero-Gil, C. Hugonie, S.F. King, D.P. Roy, S. Vempati, Phys. Lett. B 489 (2000) 359, hep-ph/0006198;
A. Delgado, C. Kolda, J.P. Olson, A. de la Puente, Phys. Rev. Lett. 105 (2010) 091802, arXiv:1005.1282 [hep-ph];
U. Ellwanger, G. Espitalier-Noel, C. Hugonie, JHEP 1109 (2011) 105, arXiv:1107.2472 [hep-ph];
G.G. Ross, K. Schmidt-Hoberg, arXiv:1108.1284 [hep-ph].

[12] P. Fayet, Nucl. Phys. B 90 (1975) 104;
P. Fayet, Phys. Lett. B 64 (1976) 159;
P. Fayet, Phys. Lett. B 69 (1977) 489;
P. Fayet, Phys. Lett. B 84 (1979) 416;
H.P. Nilles, M. Srednicki, D. Wyler, Phys. Lett. B 120 (1983) 346;
J.M. Frere, D.R. Jones, S. Raby, Nucl. Phys. B 222 (1983) 11;
J.P. Derendinger, C.A. Savoy, Nucl. Phys. B 237 (1984) 307;
A.I. Veselov, M.I. Vysotsky, K.A. Ter-Martirosian, Sov. Phys. JETP 63 (1986) 489;
J.R. Ellis, J.F. Gunion, H.E. Haber, L. Roszkowski, F. Zwirner, Phys. Rev. D 39 (1989) 844;
M. Drees, Int. J. Mod. Phys. A 4 (1989) 3635.

[13] U. Ellwanger, M. Rausch de Traubenberg, C.A. Savoy, Phys. Lett. B 315 (1993) 331;
U. Ellwanger, M. Rausch de Traubenberg, C.A. Savoy, Z. Phys. C 67 (1995) 665;
U. Ellwanger, M. Rausch de Traubenberg, C.A. Savoy, Nucl. Phys. B 492 (1997) 307;
U. Ellwanger, Phys. Lett. B 303 (1993) 271;

P. Pandita, Z. Phys. C 59 (1993) 575;
T. Elliott, S.F. King, P.L. White, Phys. Rev. D 49 (1994) 2435;
S.F. King, P.L. White, Phys. Rev. D 52 (1995) 4183;
F. Franke, H. Fraas, Int. J. Mod. Phys. A 12 (1997) 479.
[14] D.J. Miller, R. Nevzorov, P.M. Zerwas, Nucl. Phys. B 681 (2004) 3, hep-ph/0304049;
R. Nevzorov, D.J. Miller, in: N.S. Mankoc-Borstnik, H.B. Nielsen, C.D. Froggatt, D. Lukman (Eds.), Proceedings to the 7th Workshop "What Comes Beyond the Standard Model", DMFA–Zaloznistvo, Ljubljana, 2004, p. 107, hep-ph/0411275.
[15] M. Maniatis, Int. J. Mod. Phys. A 25 (2010) 3505, arXiv:0906.0777 [hep-ph].
[16] U. Ellwanger, C. Hugonie, A.M. Teixeira, Phys. Rept. 496 (2010) 1, arXiv:0910.1785 [hep-ph];
U. Ellwanger, Eur. Phys. J. C 71 (2011) 1782, arXiv:1108.0157 [hep-ph].
[17] R. Barbieri, L.J. Hall, A.Y. Papaioannou, D. Pappadopulo, V.S. Rychkov, JHEP 0803 (2008) 005, arXiv:0712.2903 [hep-ph].
[18] J.E. Kim, H.P. Nilles, Phys. Lett. B 138 (1984) 150.
[19] B.A. Dobrescu, G. Landsberg, K.T. Matchev, Phys. Rev. D 63 (2001) 075003;
B.A. Dobrescu, K.T. Matchev, JHEP 0009 (2000) 031.
[20] U. Ellwanger, J.F. Gunion, C. Hugonie, S. Moretti, arXiv:hep-ph/0305109;
U. Ellwanger, J.F. Gunion, C. Hugonie, S. Moretti, arXiv:hep-ph/0401228;
K.A. Assamagan, et al., Higgs Working Group Collaboration, The Higgs Working Group: Summary report 2003, arXiv:hep-ph/0406152;
G. Weiglein, et al., LHC/LC Study Group, Phys. Rept. 426 (2006) 47.
[21] U. Ellwanger, J.F. Gunion, C. Hugonie, JHEP 0502 (2005) 066.
[22] R. Dermisek, J.F. Gunion, Phys. Rev. Lett. 95 (2005) 041801;
R. Dermisek, J.F. Gunion, Phys. Rev. D 76 (2007) 095006, arXiv:0705.4387 [hep-ph].
[23] U. Ellwanger, J.F. Gunion, C. Hugonie, JHEP 0507 (2005) 041.
[24] R. Dermisek, J.F. Gunion, Phys. Rev. D 73 (2006) 111701;
R. Dermisek, J.F. Gunion, Phys. Rev. D 75 (2007) 075019;
S. Chang, P.J. Fox, N. Weiner, JHEP 0608 (2006) 068.
[25] P.W. Graham, A. Pierce, J.G. Wacker, arXiv:hep-ph/0605162.
[26] S. Moretti, S. Munir, P. Poulose, Phys. Lett. B 644 (2007) 241;
C. Hugonie, S. Moretti, arXiv:hep-ph/0110241.
[27] S. Chang, P.J. Fox, N. Weiner, Phys. Rev. Lett. 98 (2007) 111802.
[28] R. Dermisek, J.F. Gunion, Phys. Rev. D 75 (2007) 075019.
[29] T. Stelzer, S. Wiesenfeldt, S. Willenbrock, Phys. Rev. D 75 (2007) 077701;
U. Aglietti, et al., Tevatron-for-LHC report: Higgs, arXiv:hep-ph/0612172.
[30] K. Cheung, J. Song, Q.S. Yan, Phys. Rev. Lett. 99 (2007) 031801.
[31] G. Belanger, F. Boudjema, C. Hugonie, A. Pukhov, A. Semenov, JCAP 0509 (2005) 001;
J.F. Gunion, D. Hooper, B. McElrath, Phys. Rev. D 73 (2006) 015011;
D.G. Cerdeno, E. Gabrielli, D.E. Lopez-Fogliani, C. Munoz, A.M. Teixeira, JCAP 0706 (2007) 008;
V. Barger, P. Langacker, I. Lewis, M. McCaskey, G. Shaughnessy, B. Yencho, Phys. Rev. D 75 (2007) 115002;
C. Hugonie, G. Belanger, A. Pukhov, JCAP 0711 (2007) 009, arXiv:0707.0628 [hep-ph].
[32] See for instance: B.C. Allanach, et al., Eur. Phys. J. C 25 (2002) 113, hep-ph/0202233;
J.A. Aguilar-Saavedra, et al., Eur. Phys. J. C 46 (2006) 43.
[33] See for instance: M. Carena, S. Heinemeyer, C.E.M. Wagner, G. Weiglein, arXiv:hep-ph/9912223;
S. Heinemeyer, Int. J. Mod. Phys. A 21 (2006) 2659;
LEP Collaboration (ALEPH, DELPHI, L3, OPAL), Phys. Lett. B 565 (2003) 61.
[34] A. Djouadi, M. Drees, U. Ellwanger, R. Godbole, C. Hugonie, S.F. King, S. Lehti, S. Moretti, et al., JHEP 0807 (2008) 002, arXiv:0801.4321 [hep-ph].
[35] U. Ellwanger, C. Hugonie, Comput. Phys. Commun. 175 (2006) 290.
[36] U. Ellwanger, C. Hugonie, Comput. Phys. Commun. 177 (2007) 399, see also http://www.th.u-psud.fr/NMHDECAY/nmssmtools.html.
[37] C. Brust, A. Katz, S. Lawrence, R. Sundrum, arXiv:1110.6670 [hep-ph].
[38] M. Cvetic, D.A. Demir, J.R. Espinosa, L.L. Everett, P. Langacker, Phys. Rev. D 56 (1997) 2861;
M. Cvetic, D.A. Demir, J.R. Espinosa, L.L. Everett, P. Langacker, Phys. Rev. D 58 (1998) 119905 (Erratum);
P. Langacker, J. Wang, Phys. Rev. D 58 (1998) 115010;
C. Panagiotakopoulos, K. Tamvakis, Phys. Lett. B 446 (1999) 224;

C. Panagiotakopoulos, K. Tamvakis, Phys. Lett. B 469 (1999) 145;
C. Panagiotakopoulos, A. Pilaftsis, Phys. Rev. D 63 (2001) 055003;
A. Dedes, C. Hugonie, S. Moretti, K. Tamvakis, Phys. Rev. D 63 (2001) 055009;
A. Menon, D.E. Morrissey, C.E.M. Wagner, Phys. Rev. D 70 (2004) 035005;
T. Han, P. Langacker, B. McElrath, Phys. Rev. D 70 (2004) 115006;
D.A. Demir, G.L. Kane, T.T. Wang, Phys. Rev. D 72 (2005) 015012;
S.F. King, S. Moretti, R. Nevzorov, Phys. Lett. B 634 (2006) 278;
S.F. King, S. Moretti, R. Nevzorov, Phys. Rev. D 73 (2006) 035009;
V. Barger, P. Langacker, H.S. Lee, G. Shaughnessy, Phys. Rev. D 73 (2006) 115010;
S.F. King, R. Luo, D.J. Miller, R. Nevzorov, JHEP 0812 (2008) 042.

[39] M. Matsuda, M. Tanimoto, Phys. Rev. D 52 (1995) 3100;
N. Haba, Prog. Theor. Phys. 97 (1997) 301;
S.W. Ham, S.K. Oh, D. Son, Phys. Rev. D 65 (2002) 075004;
M. Boz, Mod. Phys. Lett. A 21 (2006) 243;
S.W. Ham, S.H. Kim, S.K. Oh, D. Son, Phys. Rev. D 76 (2007) 115013, arXiv:0708.2755 [hep-ph];
K. Cheung, T.-J. Hou, J.S. Lee, E. Senaha, Phys. Rev. D 82 (2010) 075007, arXiv:1006.1458 [hep-ph].

[40] U. Ellwanger, C. Hugonie, Eur. Phys. J. C 5 (1998) 723;
U. Ellwanger, C. Hugonie, Eur. Phys. J. C 13 (2000) 681;
V. Barger, P. Langacker, G. Shaughnessy, Phys. Lett. B 644 (2007) 361;
V. Barger, P. Langacker, G. Shaughnessy, Phys. Rev. D 75 (2007) 055013.

[41] M. Gomez-Bock, M. Mondragon, M. Mühlleitner, R. Noriega-Papaqui, I. Pedraza, M. Spira, P.M. Zerwas, J. Phys. Conf. Ser. 18 (2005) 74, arXiv:hep-ph/0509077;
M. Gomez-Bock, M. Mondragon, M. Mühlleitner, M. Spira, P.M. Zerwas, arXiv:0712.2419 [hep-ph];
A. Djouadi, Phys. Rept. 457 (2008) 1, hep-ph/0503172;
W.D. Schlatter, P.M. Zerwas, arXiv:1112.5127 [physics.hist-ph].

[42] S. Dittmaier, et al., LHC Higgs Cross Section Working Group Collaboration, arXiv:1101.0593 [hep-ph].

[43] H.M. Georgi, S.L. Glashow, M.E. Machacek, D.V. Nanopoulos, Phys. Rev. Lett. 40 (1978) 692.

[44] Including the full mass dependence: D. Graudenz, M. Spira, P. Zerwas, Phys. Rev. Lett. 70 (1993) 1372;
M. Spira, A. Djouadi, D. Graudenz, P.M. Zerwas, Phys. Lett. B 318 (1993) 347;
M. Spira, A. Djouadi, D. Graudenz, P.M. Zerwas, Nucl. Phys. B 453 (1995) 17, hep-ph/9504378;
R. Harlander, P. Kant, JHEP 0512 (2005) 015, hep-ph/0509189;
Heavy mass limit: A. Djouadi, M. Spira, P.M. Zerwas, Phys. Lett. B 264 (1991) 440;
D. Graudenz, M. Spira, P.M. Zerwas, Phys. Rev. Lett. 70 (1993) 1372;
S. Dawson, Nucl. Phys. B 359 (1991) 283;
R.P. Kauffman, W. Schaffer, Phys. Rev. D 49 (1994) 551, hep-ph/9305279;
S. Dawson, R. Kauffman, Phys. Rev. D 49 (1994) 2298, hep-ph/9310281;
M. Kramer, E. Laenen, M. Spira, Nucl. Phys. B 511 (1998) 523, hep-ph/9611272.

[45] R.V. Harlander, W.B. Kilgore, Phys. Rev. Lett. 88 (2002) 201801, hep-ph/0201206;
C. Anastasiou, K. Melnikov, Nucl. Phys. B 646 (2002) 220, hep-ph/0207004;
V. Ravindran, J. Smith, W.L. van Neerven, Nucl. Phys. B 665 (2003) 325, hep-ph/0302135;
R.V. Harlander, W.B. Kilgore, JHEP 0210 (2002) 017, arXiv:hep-ph/0208096;
C. Anastasiou, K. Melnikov, Phys. Rev. D 67 (2003) 037501, arXiv:hep-ph/0208115.

[46] S. Catani, D. de Florian, M. Grazzini, P. Nason, JHEP 0307 (2003) 028, hep-ph/0306211;
S. Catani, et al., JHEP 0307 (2003) 028, hep-ph/0306211;
S. Moch, A. Vogt, Phys. Lett. B 631 (2005) 48, hep-ph/0508265;
V. Ravindran, Nucl. Phys. B 746 (2006) 58, arXiv:hep-ph/0512249.

[47] R.V. Harlander, K.J. Ozeren, Phys. Lett. B 679 (2009) 467, arXiv:0907.2997 [hep-ph];
R.V. Harlander, K.J. Ozeren, JHEP 0911 (2009) 088, arXiv:0909.3420 [hep-ph];
A. Pak, M. Rogal, M. Steinhauser, Phys. Lett. B 679 (2009) 473, arXiv:0907.2998 [hep-ph];
A. Pak, M. Rogal, M. Steinhauser, arXiv:0911.4662 [hep-ph].

[48] A. Djouadi, P. Gambino, Phys. Rev. Lett. 73 (1994) 2528, hep-ph/9406432;
A. Ghinculov, J.J. van der Bij, Nucl. Phys. B 482 (1996) 59, hep-ph/9511414;
A. Djouadi, P. Gambino, B.A. Kniehl, Nucl. Phys. B 523 (1998) 17, hep-ph/9712330;
G. Degrassi, F. Maltoni, Phys. Lett. B 600 (2004) 255, hep-ph/0407249;
U. Aglietti, R. Bonciani, G. Degrassi, A. Vicini, hep-ph/0610033;
S. Actis, G. Passarino, C. Sturm, S. Uccirati, Phys. Lett. B 670 (2008) 12, arXiv:0809.1301;

C. Anastasiou, R. Boughezal, F. Petriello, JHEP 0904 (2009) 003, arXiv:0811.3458.
[49] S. Dawson, A. Djouadi, M. Spira, Phys. Rev. Lett. 77 (1996) 16, arXiv:hep-ph/9603423.
[50] R.V. Harlander, M. Steinhauser, Phys. Lett. B 574 (2003) 258, arXiv:hep-ph/0307346;
R.V. Harlander, M. Steinhauser, Phys. Rev. D 68 (2003) 111701, arXiv:hep-ph/0308210;
R.V. Harlander, M. Steinhauser, JHEP 0409 (2004) 066, arXiv:hep-ph/0409010;
R.V. Harlander, F. Hofmann, JHEP 0603 (2006) 050, arXiv:hep-ph/0507041;
G. Degrassi, P. Slavich, Nucl. Phys. B 805 (2008) 267, arXiv:0806.1495 [hep-ph];
G. Degrassi, P. Slavich, JHEP 1108 (2011) 128, arXiv:1107.0914 [hep-ph];
M. Mühlleitner, H. Rzehak, M. Spira, JHEP 0904 (2009) 023, arXiv:0812.3815 [hep-ph].
[51] G. Degrassi, P. Slavich, JHEP 1011 (2010) 044, arXiv:1007.3465 [hep-ph];
R.V. Harlander, F. Hofmann, H. Mantler, JHEP 1102 (2011) 055, arXiv:1012.3361 [hep-ph].
[52] C. Anastasiou, et al., JHEP 0701 (2007) 082, arXiv:hep-ph/0611236;
U. Aglietti, et al., JHEP 0701 (2007) 021, arXiv:hep-ph/0611266;
R. Bonciani, G. Degrassi, A. Vicini, JHEP 0711 (2007) 095, arXiv:0709.4227 [hep-ph].
[53] M. Muhlleitner, M. Spira, Nucl. Phys. B 790 (2008) 1, hep-ph/0612254.
[54] C. Anastasiou, S. Beerli, A. Daleo, Phys. Rev. Lett. 100 (2008) 241806, arXiv:0803.3065 [hep-ph];
M. Mühlleitner, H. Rzehak, M. Spira, PoS RADCOR2009 (2010) 043, arXiv:1001.3214 [hep-ph].
[55] A. Pak, M. Steinhauser, N. Zerf, Eur. Phys. J. C 71 (2011) 1602, arXiv:1012.0639 [hep-ph].
[56] M. Spira, HIGLU: A program for the calculation of the total Higgs production cross-section at hadron colliders via gluon fusion including QCD corrections, hep-ph/9510347.
[57] R.N. Cahn, S. Dawson, Phys. Lett. B 136 (1984) 196;
R.N. Cahn, S. Dawson, Phys. Lett. B 138 (1984) 464 (Erratum);
K.I. Hikasa, Phys. Lett. B 164 (1985) 385;
K.I. Hikasa, Phys. Lett. B 195 (1987) 623 (Erratum);
G. Altarelli, B. Mele, F. Pitolli, Nucl. Phys. B 287 (1987) 205.
[58] T. Han, G. Valencia, S. Willenbrock, Phys. Rev. Lett. 69 (1992) 3274, hep-ph/9206246;
T. Figy, C. Oleari, D. Zeppenfeld, Phys. Rev. D 68 (2003) 073005, arXiv:hep-ph/0306109;
E.L. Berger, J.M. Campbell, Phys. Rev. D 70 (2004) 073011, arXiv:hep-ph/0403194.
[59] M. Spira, Fortsch. Phys. 46 (1998) 203, hep-ph/9705337.
[60] M. Ciccolini, A. Denner, S. Dittmaier, Phys. Rev. Lett. 99 (2007) 161803, arXiv:0707.0381 [hep-ph];
M. Ciccolini, A. Denner, S. Dittmaier, Phys. Rev. D 77 (2008) 013002, arXiv:0710.4749 [hep-ph].
[61] P. Bolzoni, et al., Phys. Rev. Lett. 105 (2010) 011801, arXiv:1003.4451 [hep-ph];
R.V. Harlander, J. Vollinga, M.M. Weber, Phys. Rev. D 77 (2008) 053010, arXiv:0801.3355 [hep-ph].
[62] A. Djouadi, M. Spira, Phys. Rev. D 62 (2000) 014004, arXiv:hep-ph/9912476.
[63] W. Hollik, et al., Phys. Rev. Lett. 102 (2009) 091802, arXiv:0804.2676 [hep-ph];
T. Figy, S. Palmer, G. Weiglein, arXiv:1012.4789 [hep-ph].
[64] http://people.web.psi.ch/spira/proglist.html.
[65] S.L. Glashow, D.V. Nanopoulos, A. Yildiz, Phys. Rev. D 18 (1978) 1724;
Z. Kunszt, Z. Trocsanyi, W.J. Stirling, Phys. Lett. B 271 (1991) 247.
[66] T. Han, S. Willenbrock, Phys. Lett. B 273 (1991) 167.
[67] R. Hamberg, W.L. van Neerven, T. Matsuura, Nucl. Phys. B 359 (1991) 343;
O. Brein, A. Djouadi, R. Harlander, Phys. Lett. B 579 (2004) 149, hep-ph/0307206.
[68] M.L. Ciccolini, S. Dittmaier, M. Kramer, Phys. Rev. D 68 (2003) 073003, hep-ph/0306234.
[69] R. Raitio, W.W. Wada, Phys. Rev. D 19 (1979) 941;
J.N. Ng, P. Zakarauskas, Phys. Rev. D 29 (1984) 876;
Z. Kunszt, Nucl. Phys. B 247 (1984) 339;
J.F. Gunion, Phys. Lett. B 261 (1991) 510;
W.J. Marciano, F.E. Paige, Phys. Rev. Lett. 66 (1991) 2433.
[70] S. Dittmaier, M. Kramer, M. Spira, Phys. Rev. D 70 (2004) 074010, arXiv:hep-ph/0309204;
S. Dawson, C. Jackson, L. Reina, D. Wackeroth, Phys. Rev. D 69 (2004) 074027, arXiv:hep-ph/0311067.
[71] W. Beenakker, S. Dittmaier, M. Kramer, B. Plumper, M. Spira, P.M. Zerwas, Phys. Rev. Lett. 87 (2001) 201805, hep-ph/0107081;
W. Beenakker, S. Dittmaier, M. Kramer, B. Plumper, M. Spira, P.M. Zerwas, Nucl. Phys. B 653 (2003) 151, hep-ph/0211352;
L. Reina, S. Dawson, Phys. Rev. Lett. 87 (2001) 201804, arXiv:hep-ph/0107101;
S. Dawson, L.H. Orr, L. Reina, D. Wackeroth, Phys. Rev. D 67 (2003) 071503, hep-ph/0211438.

[72] https://twiki.cern.ch/twiki/bin/view/LHCPhysics/CrossSections.
[73] W. Peng, et al., Phys. Lett. B 618 (2005) 209, arXiv:hep-ph/0505086;
W. Hollik, M. Rauch, AIP Conf. Proc. 903 (2007) 117, arXiv:hep-ph/0610340.
[74] K. Nakamura, et al., Particle Data Group, J. Phys. G 37 (2010) 075021, and 2011, partial update for the 2012 edition.
[75] U. Ellwanger, Phys. Lett. B 303 (1993) 271, hep-ph/9302224;
T. Elliott, S.F. King, P.L. White, Phys. Lett. B 305 (1993) 71, hep-ph/9302202;
T. Elliott, S.F. King, P.L. White, Phys. Lett. B 314 (1993) 56, hep-ph/9305282;
T. Elliott, S.F. King, P.L. White, Phys. Rev. D 49 (1994) 2435, hep-ph/9308309;
P.N. Pandita, Z. Phys. C 59 (1993) 575;
P.N. Pandita, Phys. Lett. B 318 (1993) 338.
[76] U. Ellwanger, C. Hugonie, Phys. Lett. B 623 (2005) 93, hep-ph/0504269.
[77] G. Degrassi, P. Slavich, Nucl. Phys. B 825 (2010) 119, arXiv:0907.4682 [hep-ph].
[78] F. Staub, W. Porod, B. Herrmann, JHEP 1010 (2010) 040, arXiv:1007.4049 [hep-ph].
[79] K. Ender, T. Graf, M. Muhlleitner, H. Rzehak, arXiv:1111.4952 [hep-ph].
[80] A. Djouadi, M. Spira, P.M. Zerwas, Phys. Lett. B 264 (1991) 440;
A. Djouadi, M. Spira, P.M. Zerwas, Phys. C 70 (1996) 427;
M. Spira, et al., Nucl. Phys. B 453 (1995) 17;
A. Djouadi, J. Kalinowski, M. Spira, Comput. Phys. Commun. 108 (1998) 56.
[81] A. Djouadi, M.M. Muhlleitner, M. Spira, Acta Phys. Polon. B 38 (2007) 635, hep-ph/0609292.
[82] D. Das, U. Ellwanger, A.M. Teixeira, arXiv:1106.5633 [hep-ph].
[83] M. Muhlleitner, A. Djouadi, Y. Mambrini, Comput. Phys. Commun. 168 (2005) 46, hep-ph/0311167;
M. Muhlleitner, Acta Phys. Polon. B 35 (2004) 2753, hep-ph/0409200.
[84] P.Z. Skands, et al., JHEP 0407 (2004) 036, hep-ph/0311123;
B.C. Allanach, et al., Comput. Phys. Commun. 180 (2009) 8, arXiv:0801.0045 [hep-ph].
[85] G. Belanger, F. Boudjema, A. Pukhov, A. Semenov, Comput. Phys. Commun. 149 (2002) 103, hep-ph/0112278;
G. Belanger, F. Boudjema, A. Pukhov, A. Semenov, Comput. Phys. Commun. 174 (2006) 577, hep-ph/0405253;
G. Belanger, F. Boudjema, A. Pukhov, A. Semenov, Comput. Phys. Commun. 180 (2009) 747, arXiv:0803.2360 [hep-ph];
G. Belanger, et al., Comput. Phys. Commun. 182 (2011) 842, arXiv:1004.1092 [hep-ph].
[86] J. Hamann, S. Hannestad, M. Sloth, Y. Wong, Phys. Rev. D 75 (2007) 023522.
[87] S. Schael, et al., ALEPH Collaboration, DELPHI Collaboration, L3 Collaboration, OPAL Collaboration, Eur. Phys. J. C 47 (2006) 547.
[88] G. Hiller, Phys. Rev. D 70 (2004) 034018;
F. Domingo, U. Ellwanger, JHEP 0712 (2007) 090.
[89] G. Aad, et al., ATLAS Collaboration, Phys. Lett. B 701 (2011) 186, arXiv:1102.5290 [hep-ex];
G. Aad, et al., ATLAS Collaboration, Phys. Lett. B 701 (2011) 398, arXiv:1103.4344 [hep-ex];
G. Aad, et al., ATLAS Collaboration, arXiv:1109.6572 [hep-ex];
G. Aad, et al., ATLAS Collaboration, JHEP 1111 (2011) 099, arXiv:1110.2299 [hep-ex];
ATLAS Collaboration, ATLAS-CONF-2011-086, ATLAS-CONF-2011-098, ATLAS-CONF-2011-155.
[90] S. Chatrchyan, et al., CMS Collaboration, Phys. Rev. Lett. 107 (2011) 221804, arXiv:1109.2352 [hep-ex];
CMS Collaboration, CMS-PAS-SUS-11-004, CMS-PAS-SUS-11-005, CMS-PAS-SUS-11-006.
[91] G. Aad, et al., Atlas Collaboration, Phys. Rev. Lett. 106 (2011) 131802, arXiv:1102.2357 [hep-ex];
G. Aad, et al., Atlas Collaboration, Phys. Rev. D 85 (2012) 012006, arXiv:1109.6606 [hep-ex], ATLAS-CONF-2011-130;
CMS Collaboration, CMS-PAS-SUS-11-007, CMS-PAS-SUS-11-010, CMS-PAS-SUS-11-011, CMS-PAS-SUS-11-013, CMS-PAS-SUS-11-015.
[92] K. Sakurai, K. Takayama, JHEP 1112 (2011) 063, arXiv:1106.3794 [hep-ph];
R. Essig, E. Izaguirre, J. Kaplan, J.G. Wacker, JHEP 1201 (2012) 074, arXiv:1110.6443 [hep-ph];
C. Brust, A. Katz, S. Lawrence, R. Sundrum, arXiv:1110.6670 [hep-ph];
M. Papucci, J.T. Ruderman, A. Weiler, arXiv:1110.6926 [hep-ph];
X.-J. Bi, Q.-S. Yan, P.-F. Yin, Phys. Rev. D 85 (2012) 035005, arXiv:1111.2250 [hep-ph];
N. Desai, B. Mukhopadhyaya, arXiv:1111.2830 [hep-ph].
[93] K. Griest, D. Seckel, Phys. Rev. D 43 (1991) 3191;
C. Boehm, A. Djouadi, M. Drees, Phys. Rev. D 62 (2000) 035012, hep-ph/9911496;
C. Balazs, M.S. Carena, C.E.M. Wagner, Phys. Rev. D 70 (2004) 015007, hep-ph/0403224.

[94] K.i. Hikasa, M. Kobayashi, Phys. Rev. D 36 (1987) 724;
M. Muhlleitner, E. Popenda, JHEP 1104 (2011) 095, arXiv:1102.5712 [hep-ph].
[95] C. Boehm, A. Djouadi, Y. Mambrini, Phys. Rev. D 61 (2000) 095006, hep-ph/9907428.
[96] V.M. Abazov, et al., D0 Collaboration, Phys. Lett. B 665 (2008) 1, arXiv:0803.2263 [hep-ex];
T. Aaltonen, et al., CDF Collaboration, CDF Note 9834.
[97] B. He, T. Li, Q. Shafi, arXiv:1112.4461 [hep-ph];
M.A. Ajaib, T. Li, Q. Shafi, arXiv:1111.4467 [hep-ph];
J.S. Kim, H. Sedello, arXiv:1112.5324 [hep-ph].
[98] G. Hiller, Y. Nir, JHEP 0803 (2008) 046, arXiv:0802.0916 [hep-ph];
G. Hiller, J.S. Kim, H. Sedello, Phys. Rev. D 80 (2009) 115016, arXiv:0910.2124 [hep-ph];
T.J. LeCompte, S.P. Martin, Phys. Rev. D 84 (2011) 015004, arXiv:1105.4304 [hep-ph];
K. Huitu, L. Leinonen, J. Laamanen, Phys. Rev. D 84 (2011) 075021, arXiv:1107.2128 [hep-ph];
S. Bornhauser, M. Drees, S. Grab, J.S. Kim, Phys. Rev. D 83 (2011) 035008, arXiv:1011.5508 [hep-ph].
[99] Y. Kats, D. Shih, JHEP 1108 (2011) 049, arXiv:1106.0030 [hep-ph];
Y. Kats, P. Meade, M. Reece, D. Shih, JHEP 1202 (2012) 115, arXiv:1110.6444 [hep-ph];
J.S. Kim, H. Sedello, arXiv:1112.5324 [hep-ph].
[100] G. Aad, et al., ATLAS Collaboration, Phys. Lett. B 701 (2011) 1, arXiv:1103.1984 [hep-ex].
[101] U. Ellwanger, Phys. Lett. B 698 (2011) 293, arXiv:1012.1201 [hep-ph].